Timing of Neanderthal occupations in the southeastern margins of the Massif Central (France): A multi-method approach

Maïlys Richard, Edwige Pons-Branchu, Kim Genuite, Stéphane Jaillet, Renaud Joannes-Boyau, Ningsheng Wang, Dominique Genty, Hai Cheng, Gilbert Price, Monique Pierre, et al.

HAL Id: hal-03411392
https://hal.science/hal-03411392

Submitted on 9 Nov 2021

Timing of Neanderthal occupations in the southeastern margins of the Massif Central (France): A multi-method approach

Maïlys Richard [a, b, c, d], Edwige Pons-Branchu [a], Kim Genuite [e], Stéphane Jaillet [e], Renaud Joannes-Boyau [f], Ningsheng Wang [g], Dominique Genty [h], Hai Cheng [i, j], Gilbert J. Price [k], Monique Pierre [a], Arnaud Dapoigny [a], Christophe Falguères [b], Olivier Tombret [b], Pierre Voinchet [b], Jean-Jacques Bahain [b], Marie-Hélène Moncel [b]

[a] Laboratoire des Sciences du Climat et de l'Environnement, GEOTRAC-LSCE/IPSL, UMR 8212, CEA-CNRS-UVSQ, Universit´e Paris-Saclay, 91191 Gif-sur-Yvette, France

[b] Histoire naturelle de l'Homme préhistorique, UMR 7194, D´epartement « Homme et Environnement », Muséum National d'Histoire Naturelle, 75013 Paris, France

[c] Department of Early Prehistory and Quaternary Ecology, University of Tübingen, 72070 Tübingen, Germany

[d] Centro Nacional de Investigación Sobre la Evolución Humana (CENIEH), 09002 Burgos, Spain

[e] Laboratoire Environnement Dynamiques et Territoires de Montagne (EDYTEM), UMR 5204, 73376 Le Bourget du Lac, France

[f] Geoarchaeology and Archaeometry Research Group (GARG), Southern Cross University, 2480 Lismore, New South Wales, Australia

[g] School of Geography, Environment and Earth Sciences, Victoria University of Wellington, 6012 Wellington, New Zealand

[h] Environnements et Paléoenvironnements Océaniques et Continentaux (EPOC-OASU), UMR 5805, Universit´e de Bordeaux, 33615 Pessac, France

[i] Institute of Global Environmental Change, Xi'an Jiaotong University, Xi'an, 710049, China

[j] Key Laboratory of Karst Dynamics, MLR, Institute of Karst Geology, CAGS, Guilin, 541004, China

[k] School of Earth and Environmental Sciences, The University of Queensland, 4072 Brisbane QLD, Australia

Abstract: The middle Rhône valley, located at the southeastern margins of the Massif Central in France, produced a large number of Middle Palaeolithic sites, most of which dated to the Middle and Late Pleistocene. Due to its position, connecting northern Europe and the Mediterranean basin, this corridor and the surrounding plateaus are of particular interest in the study of human cultural evolution, including the emergence of Middle Palaeolithic technology around 300,000 years ago and its variability over time, as well as the subsistence and mobility strategies of Neanderthals.

In the last 20 years, several research projects undertaken in this region allowed to revise key Middle Palaeolithic sequences. This work aims at synthesising previous and new chronological data obtained by using uranium-series of speleothems and bones, infrared stimulated luminescence of feldspar and electron spin resonance of tooth enamel and quartz. We review previous ages obtained in the area and present 43 new ages that are discussed together to propose a reliable spatiotemporal framework for Neanderthal occupations.

We focus on major sites in the region: Payre, Ranc-Pointu 2, Baume Flandin, Abri du Maras, Grotte des Barasses II, Abri des Pêcheurs, Grotte du Figuier and Grotte de Saint-Marcel. They all provided significant information related to the biological and behavioural evolution of Neanderthal populations on the right bank of the Rhône valley. We present here the updated chronology for the Middle Palaeolithic of this area, ranging from ca. 300,000 to 40,000 years ago.

1. Introduction

Europe features very diverse topographical and environmental areas. Southern Europe, as opposed to the great North European plain (from Great Britain to Siberia via Ukraine), is a set of enclosed areas comprising plateaus, mountain environment, basins and valleys linked by corridors. The Rhône valley, located at the interface between Northern and Southern Europe, is a vast north-south river corridor that may have served as a dispersal route for people, objects and/or ideas (Fig. 1). The middle Rhône valley, sensu stricto, is the narrowest part of this corridor. It is bordered by a series of low plateaus separated by transverse valleys, adjacent to the foothills of the Massif Central and the Alps. The deposits, known today for documenting Middle Palaeolithic occupations, are located mainly on the right bank of the Rhône River (Fig. 1). The lack of archaeological occurrences in the Rhône valley is probably caused by continuous sedimentation and destruction linked to broad shifts in riverbed location (Mandier, 1984; Argant et al., 1991). Towards the Massif Central and the mid-mountains, the few known sites suggest that Neanderthals settled punctually in this area, but their relation to the Rhône valley has yet to be clarified. The left bank, on the Drôme side, is presently less known. However, some high-altitude sites document an organised frequentation of the alpine mountains by Neanderthals (e.g., in Vercors, Bernard-Guelle, 2005). Systematic excavations in this part of France began in the 1950s with a first synthetic study published in the late 1960s by J. Combier (1967). He proposed the hypothesis of a regional cultural zone ("Rhône facies") framed in the alpine chronology. The environmental framework was still largely to be specified and the faunal and micro-faunal analyses provided clues about mosaic environments according to cold or temperate contexts (Moncel et al., 2015). The revision of the faunal and lithic collections, new survey of raw material sources, the multiplication of environmental studies and the new excavations now make it possible to approach the question of settlement modes in this region from a new angle. It allows specifying the settlement patterns, the variability of subsistence strategies and the function of the sites in a more precise chronological framework. Since the beginning of the research in this region, several questions were raised, and directed our research objectives: (1) To which extent did the location and topography of this southern region influence the subsistence strategies, settlement history and territorial mobility of the Neanderthals and their ancestors? (2) In what way did climatic variations affect subsistence strategies, considering that these variations greatly modified the landscapes, food resources and the resilience of animal and plant species at the local level? (3) What are the technical and subsistence solutions chosen over time by human groups and can we observe specific traditions from the Middle Rhône valley compared to other areas in Europe? (4) Is there a regional substratum that persists over time or are there distinct phases of occupation?

Regional synthesis on the subsistence strategies indicate seasonal occupations of various durations opposing bivouacs to shorter and longer-term occupations between Marine Isotope Stage (MIS) 7 and 3 (Daujeard and Moncel, 2010). These types of sites are not related to specific technological behaviours, suggesting punctual recorded events of various traditions with the choice of a main core technology or the association of diverse modes of debitage (including the Rhodanian Quina facies), or can be linked to the type of activities (Raynal et al., 2013b; Moncel et al., 2014a, 2021). Most of the tool-kit is composed of few retouched flake-tools (scrapers and points) and the ratio differs according or not to the main core technology (Levallois, discoid-type).

Discussions over the issue of diversity of human groups, their complexity in terms of technology, mobility and territorial management are often limited by the lack of strong chronological data. Establishing a reliable and precise temporal framework for Palaeolithic sites beyond the range of radiocarbon can be challenging, and depends on the availability of material that can be dated. In karstic settings, the range of dating methods that can be applied for sites older than 50 ka includes uranium-series (^{230}Th/U) dating of speleothems and bones, luminescence dating of sediment, electron spin resonance (ESR) dating of quartz and combined ESR/U-series dating of tooth enamel. Each of these methods dates a particular event in the history of the site: the formation of secondary calcium carbonate (using uranium-series), sediment deposition (using infrared stimulated luminescence, IRSL, on feldspar or ESR on quartz), animal death and subsequent burial (using ESR and U-series). In the present study, these three methods were applied to precise the chronology of several Middle Palaeolithic sites that have been investigated in the last decade, most of which feature recurrent human occupations. Renewed fieldwork and revision of the faunal and lithic assemblages in this area provided new insights into Neanderthal occupation type and mobility. Occupations of different duration, which are not linked to core technologies, characterise this part of France (Moncel et al., 2010; Moncel, 2011; Daujeard et al., 2012; Moncel and Daujeard, 2012; Raynal et al., 2013a). Since 2005, fieldwork conducted in the key caves and shelters of Ranc-Pointu 2, Baume Flandin, Abri du Maras, Grotte des Barasses II, Abri des Pêcheurs and Grotte du Figuier (Figs. 1 and 2) allowed sampling for a multi-method geochronological study. In addition, new U-series analyses of a flowstone from the early Middle Palaeolithic site of Payre were performed to provide an age for the earliest phases of the Middle Palaeolithic in the area. We propose here an updated chronological framework for the Middle Palaeolithic sites on the right bank of the Rhône valley, which provides a new perspective on Neanderthal behaviour and demise in the area.

2. The Middle Palaeolithic sites of the Rhône valley: context and characteristics

The middle Rhône valley was occupied starting from the Middle Pleistocene, as attested in the Late Acheulean and early Middle Palaeolithic levels of Orgnac 3 (Moncel et al., 2011, 2012a; Michel et al., 2013). This site provided the earliest evidence of Levallois technology in the area, which is one of the markers of the beginning of the Middle Palaeolithic, around 300 ka (Michel et al., 2013). The sequence documents 10 phases of occupation, dated at the transition between MIS 9 and 8 (Masaoudi, 1995; Michel et al., 2013) and records gradual behavioural changes regarding land-use patterns, subsistence strategies and core technology (Moncel et al., 2005, 2011, 2012a). Together with Payre, this site plays an essential role in our understanding of the emergence of the Middle Palaeolithic in Europe with discoid-type core technologies and variants. Moreover, a number of sites documented the great variety of human behaviour during this period, especially during the Late Pleistocene, such as the caves of Ranc-Pointu 2, Baume Flandin, Barasses II and Le Figuier as well as the rock shelters of Maras and Pêcheurs (Figs. 1 and 2). These sites have been studied using an interdisciplinary approach to compare archaeological, geological, palaeoenvironmental and geochronological data to reconstruct Neanderthal dynamics in the region and to shed light onto Neanderthal adaptations to the landscape, climate and resources. Complex occupation patterns, including long-term residential, short-term regular hunting camp and brief stopover camp, characterise the Middle Palaeolithic settlements of this part of the Rhône valley. More detailed information for each studied sites is provided in the following sections.
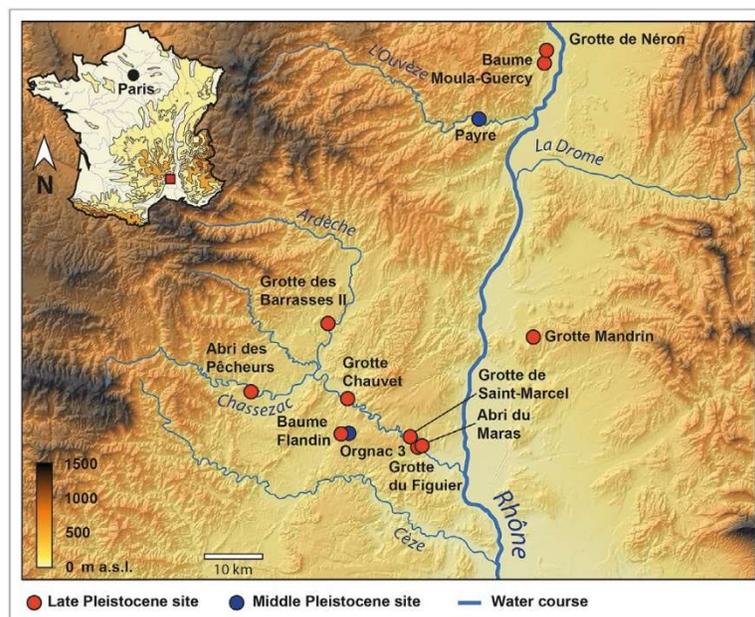
Fig. 1. Location of major Middle and Late Pleistocene sites in the middle Rhône Valley, France.
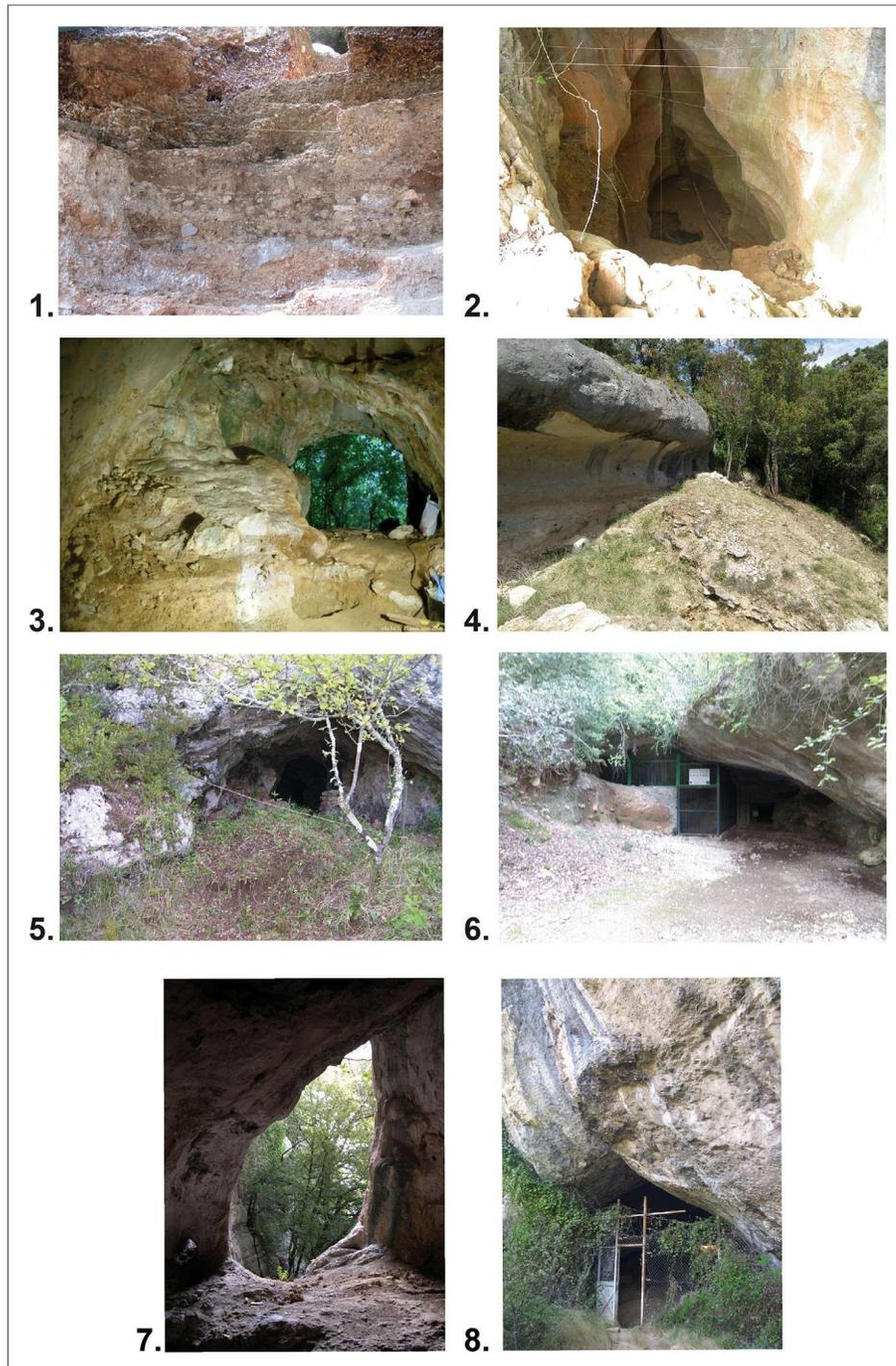
Fig. 2. Photographs of the caves and shelters occupied by Neanderthals discussed in this study: 1. Payre, a collapsed cave; 2. Abri des Pêcheurs, a narrow and deep cave; 3. Ranc-Pointu 2, a small cave; 4. Abri du Maras, a collapsed shelter; 5. Baume Flandin, a small cave; 6. Saint-Marcel, a vast cave; 7. Grotte des Barasses II, a narrow cave; 8. Grotte du Figuier, entrance of chamber 1 with a large collapse of the original entrance (M-H.Moncel).

2.1. Payre

Payre is located at the confluence of the Rhône and the Payre rivers (44° 43054.0"N 4° 44010.5"E; 170 m asl, Fig. 1). It was first excavated in the 1960s by J. Combier (1967) and by M.-H. Moncel in the 1990s and 2000s (Moncel, 2008). Payre was a cave before its roof collapsed (Fig. 2). It is today an open-air site, at least 80 m2 in surface extent, whose 5 m-thick stratigraphic sequence is composed by seven units (from bottom to top: G, F, E, D, C, B and A, Fig. 3). Four of these units feature occupation layers (G, F, D and E). A synthesis of the data obtained from the sequence is available in SOM Table S1.

The oldest archaeological units, G and F, are attributed to the early Middle Palaeolithic. The assemblage is mainly represented by scrapers and points and both discoidal and orthogonal core technologies were used on flint, attesting the variety of technological behaviours for this early phase of the Middle Palaeolithic (Chacón et al., 2016; Baena et al., 2017; Carmignani et al., 2017; Daffara et al., 2019). Some Levallois flakes were possibly introduced into the site for unit F. Flint was collected along the Rhodanian plateaus and some long-distance flint was collected over 60 km in the south (Fernandes et al., 2008). Although flint is the main raw material used, the hominins at Payre used local basalt, quartz, limestone and quartzite to knap a large heavy-duty component including some crudely-made bifacial tools (Moncel et al., 2008a, 2009; Pedergnana et al., 2018). Layer E contains large limestone blocks that correspond to a major roof collapse. Layers C and D document the last occupations, whereas layers B and A are sterile. Organic residues on flint indicate a large diversity of activities including fish and bird treatment (Hardy and Moncel, 2011).

The site is famous for providing Middle Palaeolithic layers with Neanderthal remains, bracketed between two flowstones (Fig. 3). In unit G, eight teeth, a fragment of a left parietal bone and a half-mandible were discovered, which correspond to five individuals (adults and children) (Moncel and Condemi, 1996, 1997; Grün et al., 2008; Smith et al., 2018; Verna et al., 2020).

Faunal data suggest that the site was a bear den (especially unit F) when humans were absent: *Ursus spelaeus* and *Ursus arctos* constitute 50% of the remains in unit F. Among the mammals, the most abundant species are *Cervus elaphus* ssp., *Bos primigenius* and *Equus cf mosbachensis*, which bear cut marks and were likely hunted by humans, followed by *Dicerorhinus hemitoechus* and *Elephas* sp., which could have been scavenged by both humans and carnivores (Moncel et al., 2002; Daujeard et al., 2018). The presence of species such as *Bison* sp., *Capreolus capreolus* ssp., *Megaloceros* sp., *Capra ibex*, *Hemitragus* sp., *Rupicapra* sp. and *Sus scrofa* ssp. indicates different ecosystems at the time of the seasonal occupations (shorter-term occupations in unit F compared to unit G): open in the vicinity of the cave, and forested in the valley (Moncel et al., 2002; Rivals et al., 2009; Daujeard et al., 2011; Ecker et al., 2013; Bocherens et al., 2016; Rufà et al., 2016). According to micro-faunal studies, the presence of both *Pliomys lenki* and *Microtus brecciensis* (*Iberomys*) in

layers G and D indicate a chronological range from the Middle to the beginning of the Late Pleistocene (Moncel et al., 2002; Foury et al., 2016). Palynological data indicate Mediterranean trends; however, contamination can disturb the record and cannot be excluded (Kalaï et al., 2001).

Several dating methods were applied: U-series on flowstone, ESR/U-series on teeth and bones, and thermoluminescence (TL) on flint (Masaoudi, 1995; Valladas et al., 2008). The results suggest a chronology ranging from ca. 300 ka to 140 ka (Table 1). Occupations at the base of the sequence (units G and F) would be contemporaneous with the transition between MIS 8 and 7, and the top (units D and E) with the end of MIS 6.

2.2. Ranc-Pointu 2

Ranc-Pointu 2 is a small cave located along the Ardèche River (44°200 01.1"N 4°32027.1"E; 138 m asl, Figs. 1 and 2). First excavated in the 1960s by J. Combier and in 1988 by E. Debard, they highlighted the occurrence of one archaeological layer (c1) among the five identified levels (i, h, f, c, a, from the base to the top, Fig. 3), later confirmed during fieldwork in 2008 conducted by M.-H. Moncel. The sequence is composed of both alluvial deposits and cave sedimentation that are covered by a thick flowstone.

Little material was identified in the only archaeological layer. Flakes were obtained using the unipolar Levallois core reduction method. The assemblage is dominated by sidescrapers (50%), mainly made of flint, with a few pieces in quartz and limestone (Moncel et al., 2014b). The different steps of the "chaîne opératoire" can be identified on site, and flakes with cortex were recovered, suggesting that knapping activities took place in the cave.

The faunal spectrum is dominated by cervids. *Equus* and *Rangifer tarandus* remains, found at the base of the sequence, indicate a cold and open environment. In layer c1, the presence of *Dama dama* could be related to a temperate climate. However, this taxon may be found in association with species from cold biotopes; therefore a tolerance to colder conditions cannot be excluded (Moncel et al., 2014b).

The sedimentary matrix of layer c was dated using IRSL of feldspar, providing an age of 145 ± 9 ka (Moncel et al., 2014b, Table 1).

2.3. Baume Flandin

Baume Flandin is a small cave opening to the west in a small valley in the Orgnac plateau (44°18015.8"N 4°24028.5"E; 260 m asl, Figs. 1 and 2). It is divided into two rooms, with a total surface area of 20e25 m2. It was excavated between 1954 and 1957 by L. Gauthier and C. Hugues, in 1967 by J. Combier, and in 2005 by M.-H. Moncel. The cave was emptied during earlier excavations, and for this reason the last excavation

campaign focused on the terrace. Four layers were identified (Fig. 3), from layer 4 (base) to layer 1 (top, which is composed of excavated material from the old excavations). Only layer 3 documented human occupation and can be related to the single archaeological layer found inside the cave (Moncel, 2005; Moncel et al., 2008c).

The lithic material is diversified, only cores are missing from the assemblage. Levallois and laminar technology were used to produce flakes and blades, and the site documents one of the earliest examples of laminar debitage in the south of France. Blades are produced by a volumetric debitage directly on fragments of flint slabs without preparation of the striking platform. Slabs are collected on the plateaus near the site, in the same Tertiary formations as Orgnac 3. The natural shapes of the slab are exploited and the knapping is initiated from the angles of the slab. Cores are not exhausted and the debitage stops when the flaking surface becomes too flat. The Levallois core technology only produces flakes and elongated flakes by centripetal and unipolar removals. One large bifacial element shows similarities with the handaxes uncovered in Orgnac 3 (Fig. 4, N°1). The materials excavated in the terrace and inside the cave seem to belong to the same technical tradition, and likely to the same occupation phase (Moncel et al., 2008c, 2010).

Faunal remains represent mainly large herbivores, such as cervids and equids. Forest species such as *Cervus* sp., *Capreolus capreolus*, *Dama dama* and *Sus scrofa* are also documented. The presence of *Equus* sp. and Rangifer tarandus suggests an open environment while *Capra ibex* and *Rupicapra rupicapra* are typical of a steep environment. Although carnivores are represented by *Ursus* sp. and *Canis lupus*, cut marks on long bones indicates a primary access to the carcass, likely connected to hunting activities. Deer was hunted in autumn, and bison and horses in spring, suggesting that the site was used as a seasonal camp (Daujeard et al., 2012).

2.4. Abri du Maras

Located in the Ardèche gorge, the Abri du Maras (44°18043.4"N 4°33046.2"E; 170 m asl) is a rock shelter that was first excavated in the 1950s and 1960s by R. Gilles et J. Combier (1967) (Figs. 1 and 2). Since the 2000s, excavations are conducted by M.-H. Moncel. The stratigraphy is composed by several layers, numbered from 6 (bottom) to 1 (top) (Fig. 3). Most of the archaeological material was recovered in layers 5 and 4. Cryoclastic elements were identified at the base of the sequence and indicate cold and wet conditions (layer 5 and upper 5, subdivided into three main occupation phases, 5.1, 5.2 and 5.3). The top of the sequence (layer 4, subdivided into levels 4.1 and 4.2, which are the two main phases of human occupation) is composed of silt and limestone blocks from roof collapse (Debard, 1988; Moncel et al., 2014c, 2015, 2021; Puaud et al., 2015). The latest occupations, documented at the top of the sequence, took place in a shelter configuration.

In layer 4, Levallois core technology was used for the production of flakes, blades and points, mainly from flint (Fig. 4, N°3). The Levallois core technology produced long and thin blades in situ associated to a direct laminar debitage of small nodules in the level 1 of the excavations of R. Gilles and J. Combier (Moncel, 1994, 1996; Moncel et al., 1994), at the top of the sequence. Levallois cores, on layers 4.1, 4.2 and 5-upper 5 corresponding to the lower half of the sequence, produced flakes and points by centripetal and unipolar convergent removals. Discoid-type, centripetal and unipolar cores also produced in situ flakes of small size. Refits indicate short reduction sequences in relation to short-term occupations, for instance for layer 4.1 (Moncel et al., 2021). The few blades are also produced by a Levallois core technology but the large size of some of them is incompatible with the core sizes and types found in situ, suggesting they were brought to the site. Flake-tools are rare with scrapers and convergent scrapers, including some Quina scrapers. The few Quina or "semi-Quina" are made on large flakes and the invasive "scalariform" retouch contrasts with the limited retouch of most of the flake-tools on Levallois or other types of flakes. Some small flakes look like Quina-type flakes of retouch attesting some rejuvenation of these scrapers, possibly introduced as mobile tools on the site. The largest cores were imported from a 30 km perimeter where flint was collected (Moncel et al., 2014c). The site provided major information regarding Neanderthal behaviour and cognitive capacity: fibre technology was evidenced through residue analyses (Hardy et al., 2013), in particular the identification of 3-ply cordages in layer 4.2 (Hardy et al., 2020), dated to 55 ± 2 ka to 40 ± 3 ka (Richard et al., 2015). Residues and the micro-wear analysis indicate a large diversity of activity on plants, wood and butchery (Hardy et al., 2013) and evidence of projectile is also documented by impact removals on the tip. For layer 5-upper 5, the core technologies are more diversified, and more flake-tools were uncovered, mainly made on flint coming from southern outcrops (Moncel et al., 2021). Evidence of Alnus root processing is documented in the layer 5 (Miras et al., 2020).

Regarding faunal remains, no carnivores were documented, and herbivores dominate the assemblage. *Cervus* sp., *Capreolus capreolus* and *Sus scrofa* are present at the base of the sequence, indicating a forest environment. At the top of the sequence, species such as *Rangifer tarandus*, *Bison* sp., and *Equus* cf. germanicus are the most abundant, and suggest increasingly cold conditions from the bottom to the top of the sequence (Daujeard et al., 2019b; Marín et al., 2020). No carnivore marks were identified and a great number of cut marks were observed, indicating an anthrogenic origin for the accumulation. Burnt bones, together with charcoals were also recovered in layers 4 and 5 (Moncel et al., 2021). Intensive exploitation of natural resources is consistent with a residential campsite for long-term occupation events during a whole season, mainly summer for layer 5-upper 5 (Marín et al., 2020), while for layer 4 short-term occupations took place mainly in autumn (Vettese et al., 2017; Daujeard et al., 2019b; Moncel et al., 2021).

Previous dating suggests a chronology ranging from MIS 5 to 3 for the sequence (Table 1): U-series ages on bones from layer 5 range from ca. 90 to 70 ka (Moncel and Michel, 2000). Combined ESR/U-series dating

yielded ages ranging from 90 ± 9 ka (layer 5) to 40 ± 3 ka (layer 4.1) (Richard et al., 2015), suggesting that Neanderthal populations in this area may be contemporaneous with the earliest presence of modern humans in north-western Europe (Higham et al., 2014).

2.5. Grotte des Barasses II

Located in a cliff and opening to the south, at 55 m above the Ardèche River, the Barasses II cave (44°30043.0"N 4°22012.0"E; 180 m asl) was discovered in 1966 and excavated by J. Combier et J.-L. Porte in 1967-68 (Combier, 1968) (Figs. 1 and 2). New excavations were conducted in a collective research programme between 2011 and 2013 by C. Daujeard. Two lithostratigraphic units, divided into seven stratigraphic units (from 8 to 6 for the lower part and from 5 to 2 for the upper part), were described (Daujeard, 2018) (Fig. 3).

Most of the industry was uncovered in units 2 and 3. The lithic assemblages are composed of flakes and flake-tools made on flint (Fig. 4, N°2). Few cores are present, indicating the introduction of flakes already produced. Twenty-seven different types of flint were identified, collected from alluvial deposits and colluvium from semi-local outcrops in an area extending up to 30 km from the site (Moncel et al. in Daujeard, 2018). The Levallois core technology is predominant, with the use of the centripetal and unipolar methods, and the assemblage is composed of points, burins, Levallois elongated flakes/blades and some "semi-Quina" scrapers with a scalariform and invasive retouch close to what is observed at the Abri du Maras and Grotte du Figuier. Flint is the main raw material as for most of the sites, except Abri des Pêcheurs (quartz), but some artefacts in local basalt were also found in level 6, attesting a complementary debitage of the local cobbles collected near the cave (Moncel et al. in Daujeard, 2018).

Capra ibex dominates the faunal spectrum but remains of *Equus* sp., *Cervus elaphus*, *Bison priscus*, and numerous remains attributed to carnivores (*Canis lupus*, *Vulpes vulpes*, *Felis* sp.,) including mustelids (*Martes martes*, *Mustela erminea*) and *Ursus* sp. The presence of *Microtus* (*Stenocranius*) *gregalis* at the base of the sequence suggests a cold climate, and *Pliomys lenki* and *Allocricetus bursae* remains indicate a deposition during a cold phase of the MIS 5 for the lower part of the sequence. Ibex remains appear to have been mostly accumulated naturally. The animals were either sheltered or trapped in this small and narrow cave and may have suffered secondary predator actions. There are punctual human activities with few butchery marks, observed mainly on secondary herbivore species (cervids and bovines). The cave was frequently used for sheltering, hibernating, denning or procuring food supplies by both animals and humans (Daujeard et al., 2019a; Guillaud et al., 2021). The rare anthropogenic evidence seems to be related with recurrent and short-term visits (bivouacs).

ESR/U-series ages obtained on teeth range from 111 ± 3 ka (unit 8) to 48 ± 5 ka (unit 3), indicating an

occupation time spanning from MIS 5 to MIS 3 (Richard et al., 2015; Richard in Daujeard, 2018 and Table 1). This chronology is corroborated by those obtained from the sedimentary matrix using IRSL on feldspar grains, and ages range from around 103 ± 16 ka (US 6) to 65 ± 7 ka (US 2) (Table 1).

2.6. Abri des Pêcheurs

The Abri des Pêcheurs is located on the left bank of the Chassezac, a tributary of the Ardèche River (44°24036.0"N 4°12036.0"E; 138 m asl, Fig. 1). It is a 6 m-deep sinkhole with a surface area of 20 m2 (Fig. 2). Excavations were conducted by G. Lhomme between 1973 and 1988 and by M.-H. Moncel in 2005. Occupations were attributed to the Middle and the Upper Palaeolithic (Moncel and Lhomme, 2007). A Neandertal tooth was identified in the middle part of the sequence (Bouvier, 1982).

The sequence is divided into four sectors (Fig. 3), from the base to the top: sector 4 (530-440 cm deep), sector 3 (435-395 cm), sector 2 (395-345 cm) and sector 1 (270e-50 cm) (Moncel et al., 2008b).

Lithic artefacts were mainly obtained using discoid technology, from quartz coming from local pebbles collected in the river. Quartz flaking took place on site, as indicated by the presence of discoid-type cores and unifacial cores, and various unretouched flakes and chunks (Moncel and Lhomme, 2007; Moncel et al., 2008b) including flint flakes, flake-tools and rare cores. With regard to the origin of the flint, a petrographic study indicates a wide procure-
ment perimeter oriented towards the Rhône Valley. The flint artefacts were knapped before being brought to the site, whereas local quartz was worked in the cave during short, bivouac type occupations, similar to the occupation at Barrasses II (Fernandes et al., 2008, 2010; Moncel et al., 2008b; Daujeard et al., 2012, 2019a).

Only a few anthropogenic marks were identified in the faunal remains. Indeed, the sinkhole acted as a trap for animals and was used as a den by carnivores (indicated by *Ursus spelaeus* and *Canis lupus* remains). *Capra ibex* is the most represented species. Forest species such as *Cervus elaphus* or *Capreolus capreolus* were also identified but the presence of *Rangifer tarandus* indicates a cold climate (Moncel et al., 2008b). The hypothesis of a cold climate with the persistence of forest areas near the site is strengthened by the presence of micro-mammals from cold (*Microtus oeconomus*) and forest (*Apodemus sylvaticus*) biotopes (El Hazzazi, 1998; Kalaï, 1998; Moncel et al., 2010).

A radiocarbon dating attempt in the 1980s produced an age of 29700 ± 900 years BP for the Middle Palaeolithic layers (Evin et al., 1985, Table 1). ESR and U-series dating conducted on both speleothems and bones yielded early uptake (EU) ages ranging from ca. 118 to 19 ka (Masaoudi et al., 1994, Table 1). More recently, ESR/U-series dating was applied to a tooth from layer F19 (top of the Middle Palaeolithic) and provided an age of 54 ± 5 ka (Richard et al., 2015, Table 1). A U-series age of 110 ± 15 ka was obtained from the top of a flowstone underlying the archaeological deposits (formed between the cave wall and the

sediments), thus giving a maximum age to the sequence (Richard et al., 2015, Table 1). The formation of the breccia at the base of the sequence, before the oldest Middle Palaeolithic occupations, could have thus occurred during MIS 5. The sedimentological and palynological analyses indicate deposits consistent with a cold and humid climate for the first occupations, which could belong to a pleniglacial phase (Kalaï, 1998). For the upper part of the sequence, the climate became more humid and warmer, and then a cold and dry phase is recorded, contemporaneous with the Upper Palaeolithic. Neanderthals occupied the site at the end of MIS 5 and during MIS 4. They used the deep and narrow cave for brief stops, exploiting local stones and transporting flint flakes. Like cave bears, wolves or ibex, Neanderthals used this shelter as a place of refuge where they could carry out butchering and scavenging activities.

2.7. Grotte du Figuier

The Figuier cave is located on the left bank of the Ardèche River (44°19015.7"N 4°32050.9"E; 120 m asl) and features three rooms (Fig. 1). The 8 m-high entrance is oriented to the south and opens to a first room of 150 m2 of surface area that was excavated by L. Chiron et P. Raymond at the end of the 19th and the beginning of the 20th centuries (Fig. 2). Solutrean engravings were discovered in 1906. The cave also documented human remains from the Upper Palaeolithic in rooms 1 (a child burial) and 3 (Moncel et al., 2012b). The stratigraphy described by J. Combier (1967) includes two Middle Palaeolithic layers (of which one was attributed to the Quina Mousterian) separated from the Upper Palaeolithic layers by a sterile sediment layer, spanning from the Aurignacian to the Magdalenian. The last excavations were carried out in 2007e08 by M.-H. Moncel. Correlations between stratigraphic sequences in the three rooms allow describing five layers lying on a sterile micaceous fluvial sand at the base (Fig. 3) (Moncel et al., 2010, 2012b). Layers 2 and 4 in rooms 2 and 3 provided pollens that suggest a mosaic of vegetation, mostly composed of steppic grasses (Moncel et al., 2012b).

The Middle Palaeolithic assemblages are composed of flakes, cores and side-scrapers, made mainly from local flint and quartz (Fig. 4, N°5, Moncel et al., 2012b). Past excavations in room 1 yielded two Middle Palaeolithic levels, including one with Quina facies. The Quina Rhodanian facies at Grotte du Figuier is characterised by various core technologies including discoid-types, centripetal, laminar volumetric and various other types of cores. There is no evidence of the typical "Quina core technology" described in the South-West of France (Bourguignon, 1997). Moreover, the retouch of the tools is more invasive and scalariform compared to the real Quina-type and can be described as "semi-Quina" as in the other assemblages of the same area. This facies was not recovered in rooms 2 and 3 during the recent excavations, which were located far from the current entrance. The lithic material confirms the presence of hominids with similar flaking method, such as discoid type on small flint core-flakes. Flaking took place in the three rooms and produced elongated and thick flakes. The lack of

Quina retouch suggests different types of occupations and activities in a dark area requiring fire, as evidenced by the presence of charcoal.

Regarding faunal remains, *Rangifer tarandus*, *Bison* sp. and *Equus* sp. indicate a cold climate. *Capra ibex* and *Rupicapra rupicapra* are also present. Carnivores such as *Ursus spelaeus*, *Crocuta spelaea*, *Vulpes vulpes* and *Canis lupus* were documented and, in rooms 2 and 3, *Ursus arctos*, *Panthera pardus*, *Lynx spelaea* and *Felis sylvestris*. Scavenging activities on carcasses left by carnivores indicate that the cave was alternately occupied by both carnivores (as a den) and humans (as a regular short-term camp) (Daujeard and Moncel, 2010; Moncel et al., 2010, 2012b).

Previous dating of layer 4 (room 1) to 52 ± 9 ka (Richard et al.,2015, Table 1) suggests occupation during MIS 4, as in Abri du Maras (Crégut-Bonnoure et al., 2010; Moncel et al., 2010; Moncel et al., 2012b). Gradual climate cooling, inferred from the disappearance of Dama dama, Cervus elaphus and Sus scrofa in the upper levels, does not appear in the pollen record.

2.8. Grotte de Saint-Marcel

Saint-Marcel is a cave located on the left side of the Ardèche River, in Saint-Marcel d'Ardèche, not far from the Abri du Maras, Ranc-Pointu 2 and Grotte du Figuier (44°19057.4"N 4°32026.9"E; 100 m asl, Fig. 1). It is a vast karstic network with evidence of Middle Paleolithic occupations (Fig. 2). Under the entrance, the excavations of R. Gilles from 1974 to 1988 revealed a 6.50 m-thick infill, corresponding to detrital cones built up as a result of the collapse of the entrance (Debard, 1988). Stratigraphic and sedimentological studies allowed the identification of about forty layers, grouped into two large complexes (upper and lower complexes, Fig. 3). The upper complex (layers u to c) contains several Mousterian levels. The layers can be grouped into four sedimentary sequences separated by a hiatus. Seven climatic sub-phases were identified throughout the sequence, with archaeological evidence (levels u to c) and sedimentation gaps. Levels u to k (from the bottom to the upper layer) correspond to MIS 5e-a according to biochronology (Crégut-Bonnoure et al., 2010). The upper part of the sequence was deposited during a temperate and wet period (beginning of MIS 3). Levels f to c belong to the Late Middle Palaeolithic. Human occupation is recurrent throughout the sequence and, except for level u at the bottom, no behavioural change was highlighted despite sedimentary breaks. Conventional radiocarbon bulk sample dates carried out in the 1980s on layers e and g were considered too young (ca. 23000-29000 years BP, Evin et al., 1985). In layer f, three bones from red deer bearing cut marks were collected. Two of the bones produced statistically identical results (Szmidt et al., 2010), 37850 ± 550 years BP (OxA-19623) and 37850 ± 600 years BP (OxA-19625). The third one overlaps these at two standard deviations: 41300 ± 1700 years BP (OxA-19624). Based on these results, as well as sedimentological evidence, the upper layers can be attributed to the Late Mousterian (Szmidt et al.,

2010).

Regarding microfauna, only remains found in level u at the bottom of the sequence were studied. The species are *Pitymys subterraneus*, *Apodemus sylvaticus*, *Mustella ermine* and *Talpa europaea*. They indicate the presence of meadows near forested areas related to a wet temperate climate (Debard, 1988). For the malacofauna, remains from level u are typical of a karstic context during humid climatic phases (*Vitrea* cf. *crystalline*, *Vitrea* cf. *narbonnensis*, *Caecilioides acicula*, *Clausilia* sp., *Cyclostoma elegans*). In levels p, n, m, j, i, h, g and f, all charcoals are from Pinus silvestris. *Pinus nigras salzmannii* was only identified in levels h, g and f (Debard, 1988), suggesting continental influences and thus wood gathering in a Mediterranean climate. No remains from deciduous trees were discovered.

Throughout the sequence, the faunal collection is largely dominated by cervids. Above level u, red deer (*Cervus elaphus*) is the most abundant taxon, followed by roe deer (*Capreolus capreolus*), fallow deer (*Dama dama*), ibex (*Capra caucasica prepyrenaica*), megaloceros (*Megaloceros giganteus*), horse (*Equus germanicus*), aurochs (*Bos primigenius*), European ass (*Equus hydruntinus*) and wild boar (*Sus scrofa*). Carnivore remains are absent. This association indicates temperate and humid climatic conditions with a mosaic of forest, open grasslands and rocky environments (Moncel and Daujeard, 2012). Seasonality indexes show that red deer were hunted all year round with most slaughters occurring during the autumn, mainly with young animals and adults killed in herds (Moncel et al., 2004; Daujeard and Moncel, 2010). The levels yielded a large number of bone retouchers (>300), which indicate the extensive use of bones as tools in situ. The density of the material (lithics >100/m^2), the variety of activities and the intensive exploitation of carcasses processed and consumed in the dwelling suggest a succession of long-term residential camps.

Lithic analyses reveal a consistent technical behaviour over time based on a discoid core technology on flint flakes, and occasionally on nodules and pebbles. The flint was collected from the northern and southern plateaus and along the Rhône Valley. Tools are rare and include side-scrapers and points (Fig. 4), contrasting with the high quantity of bone retouchers found all over the sequence. The retouch is marginal and does not modify the shape of the products (Moncel et al., 2004).
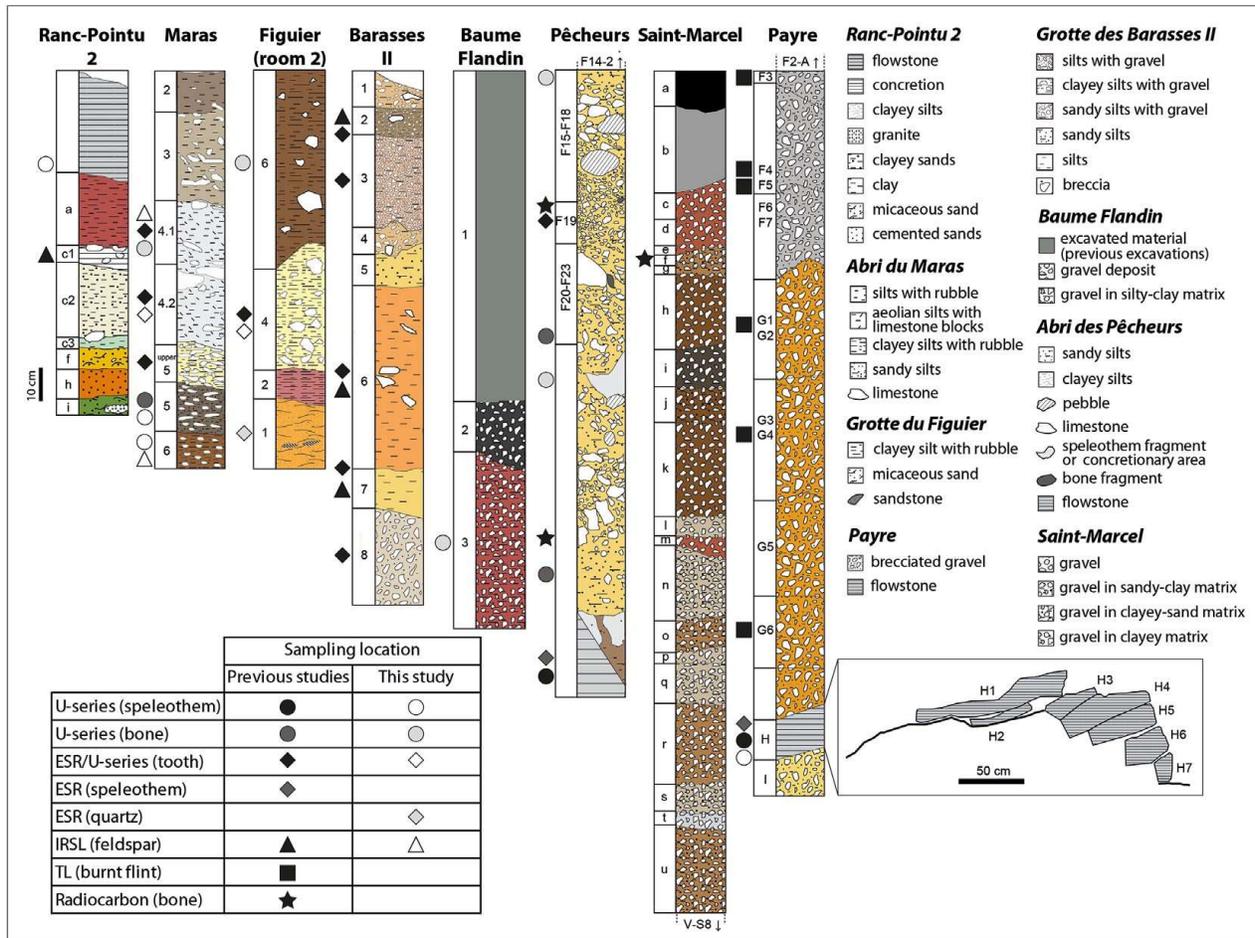
Fig. 3. Stratigraphic columns of Ranc-Pointu 2 (modified from Moncel et al., 2014b), Abri du Maras (modified from Moncel et al., 2015), Grotte du Figuier (modified from Moncel et al., 2012b), Grotte des Barasses II (modified from Daujeard, 2018), Baume Flandin (modified from Moncel et al., 2010), Abri des Pêcheurs (modified from Moncel et al., 2015), Grotte de Saint-Marcel (modified from Debard, 1988; Moncel et al., 2015) and Payre (modified from Moncel et al., 2009). The sampling position from previous studies (dark color) and this study (light color) is approximate.

Tab. 1. Previous ages obtained using U-series, thermoluminescence (TL), infrared stimulated luminescence (IRSL), combined electron spin resonance and U-series (ESR/U-series) and radiocarbon on the Middle Palaeolithic sites of the area. For ESR/U-series age calculation, EU refers to early uptake, model that assumes a rapid U uptake in the sample and a closed system during burial.

Site	Level	Sample #	Method / Material	Age (ka)	Reference
Payre	D	I6 182	ESR/U-series / teeth and bones	140 +40/-34	Valladas et al. (2008)
	D	L8 210		186 +45/-33	
	D	L8 219		139 ± 16	
	D	Tooth 3		145 +33/-23	
	D	Tooth 4		144 +31/-22	
	E	K6 8		145 +37/-27	
	E	L7 230		146 +34/-26	
	F	L6 30		227 +49/-45	
	F	M6 256		223 +59/-58	
	F	M6 303		272 +69/-65	
	G	O5 471		265 +59/-54	
Payre	F	Pay3	TL / burnt flint	213 ± 16	Valladas et al. (2008)
	F	Pay23		257 ± 20	
	F	Pay26		264 ± 19	
	F	Pay27		280 ± 25	
	F	Pay28		242 ± 20	
	G	Pay4		161 ± 14	
	G	Pay5		225 ± 16	
	G	Pay6		252 ± 19	
	G	Pay10		271 ± 19	
	G	Pay11		339 ± 40	
	G	Pay12		210 ± 13	
	G	Pay14		279 ± 21	
Payre	H1	PC94-01	U-series (alpha	135 +10/-9	Masaoudi (1995)
	H2	PC94-02		216 +26/-20	

Site	Layer	Sample	Method / Material	Age (ka)	Reference
	H3	PC94-03	spectrometry) / flowstone	253 +32/-24	
	H4	PC94-04		281 +74/-42	
	H5	PC94-05		230 +23/-19	
Payre	H1	PC94-01	ESR (EU) / flowstone	132 ± 15	Masaoudi (1995)
	H4	PC94-04		253 ± 26	
Payre	H1	H1	U-series (TIMS) / flowstone	229 ± 2	Valladas et al. (2008)
	H3	PL H3		291 ± 3	
	H5	PL H5a		280 ± 3	
Ranc Pointu 2	c1	WLL921	IRSL / feldspars	145 ± 9	Moncel et al. (2014b)
Grotte du Figuier	4 (room 1)	FIG 2010-18	ESR/U-series / teeth	52 ± 9	Richard et al. (2015)
Abri du Maras	5	AM-C5-K4-107	U-series (alpha spectrometry) / bones	87 ± 5	
	5	AM-C5-L1-116		89 ± 4	
	5	AM-C5-L3-134		91 ± 4	
	5	AM-C5-M2-155		72 ± 3	
Abri du Maras	4.1	AM L6-221	ESR/U-series / teeth	46 ± 3	Richard et al. (2015)
	4.1	AM L6-229		40 ± 3	
	4.2	AM L6-769		42 ± 3	
	4.2	AM G6-203		46 ± 6	
	4.2	AM J6-393		55 ± 2	
	upper5	AM F6-47		90 ± 9	
Abri du Maras	5	AM-C5-K4-107	U-series (alpha spectrometry)	87 ± 5	Moncel & Michel (2000)
	5	AM-C5-L1-		89 ± 4	

		116	/		
	5	AM-C5-L3-134	bones	91 ± 4	
	5	AM-C5-M2-155		72 ± 3	
Grotte des Barasses II	2/3	BA F12-A36	ESR/U-series / teeth	59 ± 6	Richard et al. (2015)
	3	BA F12-A97		61 ± 5	
	3	BA G12-42		48 ± 5	
	8	BA F13-C51		111 ± 13	
Grotte des Barasses II	6	BA F12-20053	ESR/U-series / teeth	79 ± 8	Richard in Daujeard (2018)
	6	BA F12-20100		107 ± 13	
	6/7	BA F12-20185		89 ± 6	
Grotte des Barasses II	2	WLL990	IRSL / feldspars	65 ± 7	Rué and Raynal in Daujeard (2018)
	6	WLL991		103 ± 16	
	7	WLL1040		75 ± 12	
Abri des Pécheurs	-	Ly-2340	Radiocarbon / bones	29.7 ± 0.9 (uncal. BP)	Evin et al. (1985)
	-	Ly-2342		24.9 ± 0.7 (uncal. BP)	
Abri des Pécheurs	F23	PECH 3	U-series (alpha spectrometry, EU) / bones	24 ± 1	Masaoudi et al. (1994)
	F23	PECH 4		24 ± 1	
	S5 base	PECH 5		19 ± 1	
	S5 base	PECH 6		23 ± 1	
	S5	PECH 7		27 ± 2	

|					
	base				
	S5	PECH 8		37 ± 2	
	base				
Abri des Pêcheurs	L1	PECHCA 1	U-series (alpha spectrometry) /	83 ± 6	Masaoudi et al. (1994)
	5 base	PECHCA2	flowstone	113 +7/-6	
Abri des Pêcheurs	F19	AP D5-18	ESR/U-series / Teeth	54 ± 5	Richard et al. (2015)
Abri des Pêcheurs	L1	PECHCA 1	ESR (EU) / flowstone	95 ± 14	Masaoudi et al. (1994)
	5 base	PECHCA2		118 ± 19	
Abri des Pêcheurs	Base	AP PS1	U-series (MC-ICP-MS) / flowstone	400 ± 24	Richard et al. (2015)
	Top	AP PS2	U-series (alpha spectrometry) / flowstone	110 ± 15	
Saint-Marcel	f	OxA-19623	Radiocarbon / bone	37,850 ± 550 years (uncal. BP) 42,041–42,826 years cal BP	Szmidt et al. (2010)
	f	OxA-19624		41,300 ± 1700 years (uncal. BP) 43,491–46,512 years cal BP	
	f	OxA-19625		37,850 ± 600 years (uncal. BP) 42,011–42,864 years cal BP	
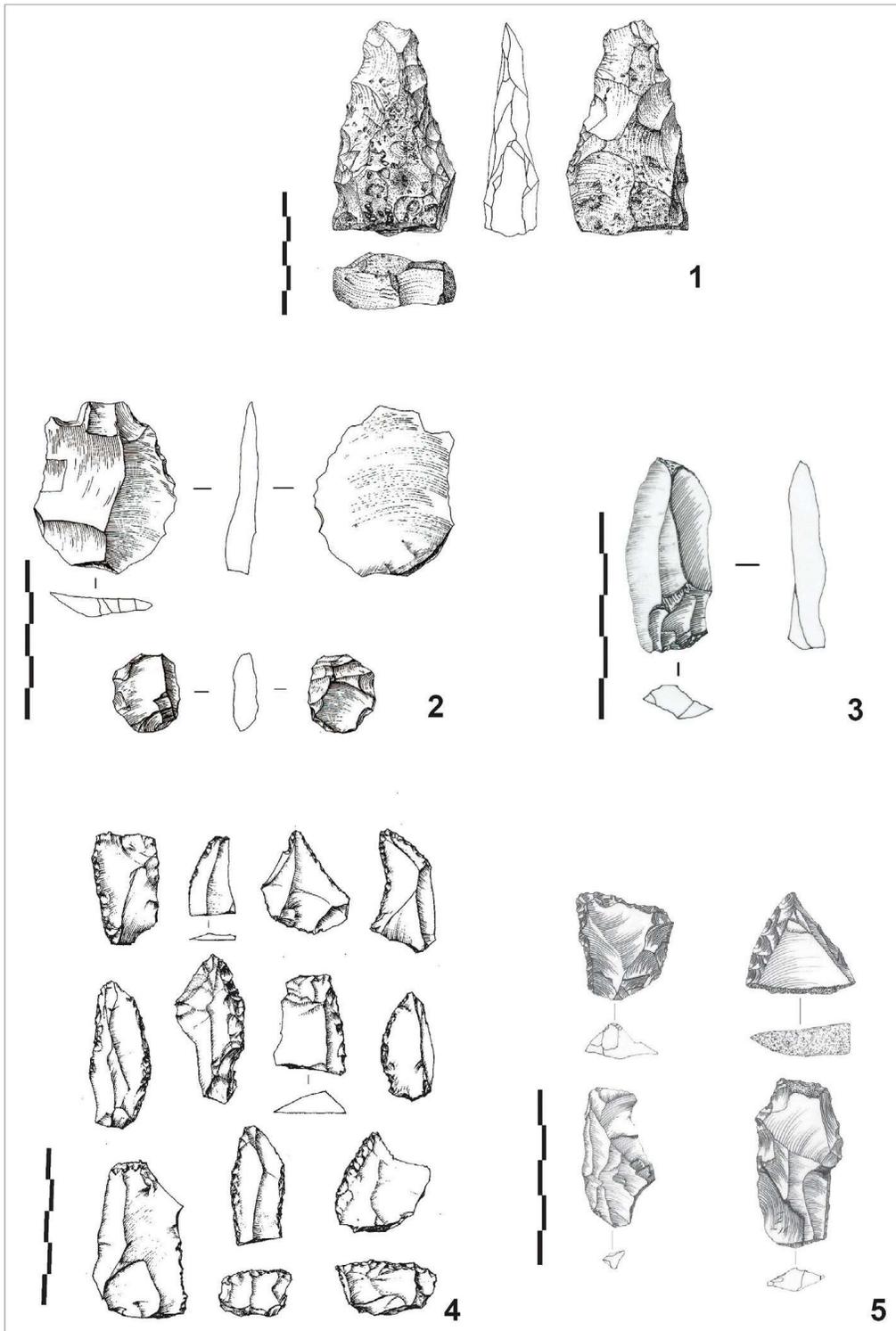
Fig. 4. Some examples of Middle Palaeolithic artefacts: 1. Partial biface on flint slab at the Baume Flandin (level 3); 2. Flint flakes from Grotte des Barasses II (upper and lower units); Flint elongated flake from the Abri du Maras (level 4.2); 4. Flint flakes from Grotte de Saint-Marcel (level i); 5. Flint scrapers from Grotte du Figuier (rooms 2 and 3). Drawings 1; 2; 3; 5: A. Theodoropoulou; 4: R. Gilles).

3. Material and methods

3.1. U-series

U-series dating (^{230}Th/U) is a method based on the radioactive decay of ^{234}U in ^{230}Th and ^{238}U in ^{234}U in the ^{238}U decay chain. At the time of the formation, calcium carbonate incorporates uranium, which is soluble in natural water, unlike thorium. ^{230}Th formed in the material is thus the daughter product of ^{234}U, and the age is given by measuring isotopic ratios ^{234}U/^{238}U and ^{230}Th/^{234}U. The method can be applied to a wide range of materials, including speleothems, corals as well as fauna and human remains (Ivanovich and Harmon, 1992). It is also combined with electron spin resonance (ESR) in teeth to derive the dose rate (Grün et al., 1988). Methodological improvements over the last fifteen years allowed increasing the precision of the dating results, with the development of inductively coupled plasma-mass spectrometry (ICP-MS). However, the method is accurate only if the dated material preserved its pristine structure and behaves as a closed system, i.e., i) it has not exchanged U and Th isotopes after the formation (for calcium carbonates) or burial (for bones and teeth); ii) U has been incorporated at the time of the formation/burial; iii) measured ^{230}Th is the product of the U decay. The main issues affecting speleothems are exogeneous Th contamination during crystallisation, dissolution and recrystallisation processes (Toffolo, 2021), which induce U leaching and thus age overestimation (e.g., Pons-Branchu et al., 2020). For bones and teeth, U is incorporated during burial; if not combined with ESR, the method provides a minimum age if U leaching is not detected (Grün et al., 2014).

For this study, four different laboratories were involved for U-series dating. The Laboratory for Science of Climate and Environment (LSCE, Gif-sur-Yvette, France) produced data on Abri du Maras (soda straw stalactites) and Ranc-Pointu 2 (flowstone), the Geoarchaeology and Archaeometry Research Group (Southern Cross University, Lismore, Australia) and the Radiogenic Isotope Laboratory (University of Queensland, Brisbane, Australia) dated bones from Baume Flandin, Abri du Maras, Abri des Pêcheurs and Grotte du Figuier, and the Institute of Global Environmental Change at Xi'an Jiaotong University (China) performed analyses on Payre (flowstone).

3.1.1. Flowstones (Payre and Ranc-Pointu 2)

Four flowstones were sampled, one from Payre and three from Ranc-Pointu 2 (Table 2).

The flowstone from Payre is the most ancient deposit, formed on the limestone substratum and located on the western side of the cave. It underlies layer G, thus providing a maximum age (terminus post quem) for the early Middle Palaeolithic occupation (Fig. 3). It is subdivided into nine units, H1 (top) to H9 (base) (SOM Fig. S1). Powder subsamples (n = 7) of 50-100 mg were drilled on a polished surface. The procedure to separate uranium and thorium was referred to in Edwards et al. (1987) and Cheng et al. (2013). Measurements

were performed on a multi-collector inductively coupled plasma mass spectrometer (MC-ICP-MS) (Thermo Scientific Neptune) at the Xi'an Jiaotong University (China).

For Ranc-Pointu 2, three samples were taken from two residual flowstones (sample RCP1 and RCP3) and from a large flowstone overlying archaeological level c (sample RCP2) (SOM Fig. S2), covering the archaeological sequence and thus providing a terminus ante quem for the underlying deposits. Samples were prepared at the LSCE according to the chemical procedure detailed in SOM. U and Th fractions were combined for the measurement on a MC-ICP-MS Thermo Scientific TM Neptune Plus fitted with a jet pump interface and a desolvating introduction system (aridus II) following Pons-Branchu et al. (2014).

3.1.2. Soda straw stalactites (Abri du Maras)

Soda straw stalactites are speleothems resulting from water dripping, forming on the cave ceiling. Due to their thin tubular morphology (see examples in SOM Fig. S3), they are fragile and generally break after a short period of time (from years to a few hundred years). They are subsequently incorporated into the sediment, providing a maximum age for the archaeological deposit (e.g., St Pierre et al., 2009; St Pierre et al., 2012). Two conditions are required to use this material as a chronometer: i) a short life span and ii) a closed system to avoid age overestimation.

Soda straw stalactites were selected from layers upper 5 and 6 (n = 17, Table 2 and Fig. S3) and the analyses were conducted at the LSCE. Samples were first rinsed with water in an ultrasonic bath and then dried in an oven. The external part of the soda straw contaminated by sediment was removed using an electric drill. The chemical procedure for the extraction and purification of uranium and thorium isotopes and the isotopic analysis using MC-ICP-MS were performed according to the procedure described above and in SOM for the flowstone from Ranc-Pointu 2.

3.1.3. Bones (Baume Flandin, Abri du Maras, Abri des Pêcheurs and Grotte du Figuier)

Bones and teeth (n = 9) were sampled for U-series dating (Table 2) by extracting powder material using a micro-drill and measured by multi-collector inductively-coupled plasma mass spectrometry at the Radiogenic Isotope Laboratory, University of Queensland, following the protocol described in Price et al. (2015). Separation and purification of U and Th isotopes was conducted using standard ion-exchange methods (Edwards et al., 1987). Details on the chemical protocol are given in SOM. UeTh fractions were combined for the measurement of isotopic ratios using a MC-ICP-MS Nu Plasma, following an analytical protocol modified from Hellstrom (2003) (see details in SOM). Baume Flandin bone was screened by LA-ICPMS to assess for diagenetic effect and diffusion pattern (Grün et al., 2008) with specific parameters at 110 mm spot size, 5 mm/s translation speed, 20 Hz frequency, and 13.1 kJ/cm^2 ablation energy (see Price et al., 2017 for method details). UeTh ages were calculated using the Isoplot/EX 3.0 program (Ludwig, 2003).

3.2. Trapped-charge dating

Unlike radiometric dating methods based on long-lived radioactive isotopes such as radiocarbon or uranium-thorium, infrared stimulated luminescence (IRSL) of feldspar and electron spin resonance (ESR) of quartz and carbonate hydroxyapatite from tooth enamel rely on the radioactive environment of the sample (i.e., the sedimentary context) and the radioactive content of the sample itself (i.e., potassium content for feldspar and uranium content for teeth). These methods are based on the property of the mineral (feldspar for IRSL, quartz and carbonate hydroxyapatite for ESR) to record a dose of ionising rays produced from radioactive decays in the sample and the sediment, and from cosmic rays. Both methods are based on a radio-sensitive signal whose intensity is a function of the ambient radioactivity and the burial time of the samples. These minerals can be dated by dividing the total dose absorbed by the sample since burial (the "equivalent dose") by the annual dose (or "dose rate") measured in the field and in the laboratory. However, the main difference between IRSL and ESR lies in the determination of the signal intensity from which the equivalent dose is calculated, i.e. using infrared stimulation for IRSL and a microwave stimulation in an induced magnetic field for ESR. The techniques to derive the dose rate (composed of alpha, beta, gamma and cosmic contributions) remain the same for both dating methods. The beta and alpha dose rates are obtained from the measurement of U, Th and K isotopes in a sediment sample using gamma-ray spectrometry and the gamma dose rate is preferentially measured in situ using a portable gamma-ray spectrometer and/or dosimeters. Nonetheless, in teeth, the uptake of uranium follows different modes and can significantly affect the dose rate. For this reason, ESR is generally combined with U-series to model the U-uptake (Grün et al., 1988). The cosmic rays are attenuated by the rock and sediment cover above the samples. The cosmic dose rate is calculated according to the sample depth below the surface along with its longitude, latitude and altitude according to the equations by Prescott and Hutton (1994).

3.2.1. Infrared stimulated luminescence dating, IRSL (Abri du Maras)

IRSL dating is commonly used to date archaeological and geological deposits, since feldspar grains contained in the sediment produce blue emissions when stimulated using infrared light (Huntley et al., 1991). The method relies on the condition that the feldspar IRSL signal was bleached by sunlight before deposition; otherwise, the presence of a residual dose causes age overestimation.

Sediment samples from Abri du Maras (n = 3) were collected using a lightproof tube inserted in the section. IRSL analyses on the fine grain polymineral fraction (4-11 mm) were carried out at the Luminescence Dating Laboratory of Victoria University of Wellington (New Zealand). Sediment at the two ends of the tube (exposed to light during sampling) was used for gamma spectrometry analyses and water content

measurement. The sediment from the centre of the tube was kept for equivalent dose determination. The details of the procedure for sample preparation and measurement are provided in the SOM.

The equivalent doses were obtained using the multiple aliquot additive dose method (MAAD). After an initial test measurement, 30 aliquots were beta irradiated in six groups up to five times of the dose result from the test, 9 aliquots were alpha irradiated in three groups up to 3 times the dose result from the test. These 39 aliquots plus 9 unirradiated aliquots were stored in the dark before measurement. Measurements were conducted using a Risø TL-DA-15 reader equipped with infrared diodes at 880 nm used to deliver a stimulated beam (30 mW/cm2) at room temperature for 100 s after a preheating of 5 min at 230°C. The blue luminescence signal centred around the 410 nm emission from feldspar was detected by an EMI 9235QA photomultiplier with a combination of two filters (Schott BG-39 and Kopp 5e58). The luminescence growth curves (exponential fitting) were constructed using the initial 10 s of the shine down curve and subtracting the average of the last 20 s. Equivalent doses were obtained by extrapolation of the growth curve to the dose axis. The shine plateau was checked to be flat after this manipulation. A similar plot for the alpha-irradiated aliquots allows an estimate of the a-efficiency, the a-value. The a-value was calculated comparing the luminescence induced by alpha irradiation with that induced by beta or gamma irradiation. The fading test was conducted following the method proposed by Huntley and Lamothe (2011). No fading trend was observed.

The environmental dose rates were obtained using the conversion factors of Adamiec and Aitken (1998), taking into account ^{238}U, ^{232}Th and ^{40}K contents measured using high resolution low-background gamma ray spectrometry with high-purity germanium detector (HPGe), water content (water/dry mass of sediment %) considering a 10% uncertainty and the a-value. Measured water content values of 16% (WLL922), 14% (WLL923) and 22% (WLL924) were used for age calculation. The cosmic dose rate was calculated using the equations from Prescott and Hutton (1994). A thickness of 9.2 m (WLL922, 70 ± 4 µGy·a-1), 8.5 m (WLL 923, 75 ± 4 µGy·a-1) for layer 4.1 and of 10.8 m (WLL 924, 60 ± 3 µGy·a-1) for layer 6 was considered.

3.2.2. Combined electron spin resonance/uranium-series of tooth enamel (Abri du Maras and Grotte du Figuier)

Grün et al. (1988) proposed to combine ESR and U-series on teeth to reconstruct the dose rate in the dental tissues that are affected by uranium uptake during diagenesis (e.g., Rae and Ivanovich, 1986). This method was successfully applied in the region to samples from the Abri du Maras, Grotte du Figuier, Grotte des Barasses II and Abri des Pêcheurs (Richard et al., 2015 and SOM Table S2). Four additional teeth were sampled from Abri du Maras (n = 2, SOM Fig. S4) and Grotte du Figuier (n 2, SOM Fig. S5) (Table 2). They were prepared and analysed following the procedure for ESR and U-series described in Richard et al. (2015). Sediment (~100 g) was collected for the calculation of the beta dose rate. Water (wet weight %) in sediments causes the attenuation of the dose rate, and it was evaluated by weighing the samples before

and after drying in an oven for 1 week at 40 °C. A value of 15 ± 5% was used for the samples from Abri du Maras and of 10 ± 5% for the samples from Grotte du Figuier. For the dental tissues, a water content (weight %) of 0% for the enamel and of 7 ± 5% for the dentine was assumed.

For the equivalent dose determination, ten powdered enamel aliquots were irradiated at increasing doses (from 32 to 2000 Gy) using a ^{137}Cs gamma source (Gammacell, CENIEH, Burgos, Spain) for the samples from Abri du Maras and nine aliquots were irradiated (from 36 to 1366 Gy) using a 60Co source (panoramic irradiation, LABRA, CEA, Saclay, France) for the samples from Grotte du Figuier. One was kept intact to measure the natural ESR signal. The carbonate hydroxyapatite T1-B2 signal (Grün, 2000) was measured with an EMX Bruker ESR spectrometer working at room temperature (19 °C) at the National Museum of Natural History (Paris, France) with the following parameters: 1 mW microwave power, 0.1 mT modulation amplitude, 12 mT scan range, 2 min scan time and 100 kHz modulation frequency. The measurements were repeated four times for each aliquot. The mean value of ESR intensity and associated standard deviation calculated from the four measurements were plotted as a function of their radiation dose using Origin Pro 8 (Origin Lab Corporation, Northampton, USA). The dose response curves were obtained using a single saturation exponential (SSE) function (Yokoyama et al., 1985) and weighted by the inverse of the squared ESR intensity (1/I2). The equivalent doses were obtained by extrapolation.

Regarding the dose rate, the contribution from alpha particles from the sediment and the dentine was eliminated by removing at least 30 mm from each side of the enamel using a dentist drill. The beta dose rate was derived from the measurement of [238]U, [232]Th and K using high resolution low-background gamma-ray spectrometry and the conversion factors of Adamiec and Aitken (1998) available in the DATA programme (Grün, 2009). The gamma dose rate was measured in situ using a portable gamma-ray multichannel analyser connected to a NaI (Tl) probe Inspector 1000 (Canberra). The measurements were performed as close as possible to the initial sampling location and the spectra were processed following the "threshold" technique (Mercier and Falguères, 2007).

The cosmic dose rate is attenuated by the cave or rock shelter roof and deposits covering the samples. It was calculated considering the limestone and sediment thickness above the samples according to the equations of Prescott and Hutton (1994). A thickness of 11 ± 2 m (57 ± 10 μGy·a-1) and 9 ± 2 m (70 ± 12 μGy·a-1) were considered for AM L11-412 and AM M10-369 respectively. For the Figuier samples, a thickness of 30 ± 1 m (19 ± 1 μGy·a-1) was used.

Ages were calculated with 1σ error range using the DATA programme (Grün, 2009) that takes into account an alpha efficiency of 0.13 ± 0.02 (Grün and Katzenberger-Apel, 1994) and Monte-Carlo beta attenuation factors from Brennan et al. (1997).

3.2.3. Electron spin resonance of quartz (Grotte du Figuier)

Two samples from alluvial deposits were collected from layer 1 at the base of the sequence in room 2 of the Figuier cave in 2010. Burial ages were calculated using the ESR signal on quartz, since the layers provided no archaeological remains. The method allows the determination of an age by measuring both aluminium (ESR-Al) and titanium (ESR-Ti-Li) radiosensitive centres (Yokoyama et al., 1985; Voinchet et al., 2004; Duval, 2012; Duval and Guilarte, 2015).

The analyses were performed at the MNHN following Genuite et al. (2021). The quartz grains were extracted following the procedure described in Voinchet et al. (2004) and were divided into 11 aliquots. One was exposed to light for 1600 h in a Honle© SOL2 solar simulator (light intensity between 3.2 and $3.4 \cdot 10^5$ Lux) to determine the unbleachable component of the ESR-Al signal (Voinchet et al., 2004). The 10 remaining aliquots were irradiated at increasing dose intensity (150, 300, 600, 1200, 2400, 4000, 6000, 8000, and 12000 Gy) using a γ 137Cs source (Gammacell, CENIEH, Burgos, Spain) to determine the equivalent dose. Intensity values of the ESR signal were measured using an EMX Bruker ESR spectrometer working at low temperature (between 105 and 112 K) at the MNHN. The multiple paramagnetic centres (MC) approach was used (Toyoda et al., 2000; Tissoux et al., 2007; Burdette et al., 2013; Duval and Guilarte, 2015). However, the Ti-H centre cannot be used for age calculation because of the high variability of the measurements (see Genuite et al., 2021). For the Al centre, measurements were performed between the top of the first peak (g = 2.018) and the base of the sixteenth peak (g = 2.002) (Duval et al., 2015). Following Toyoda et al. (2000), the ESR intensity of the Ti-Li signal was assessed by measuring the peak-to-baseline amplitude at around g = 1.913-1.915. Each aliquot was measured nine times with the following parameters: a microwave power of 5 mW; a point resolution of 1024; a sweep width of 20 mT; a modulation frequency of 100 kHz; a modulation amplitude of 0.1 mT; a conversion time of 40 ms; a time constant of 20 ms and 1 scan. The signal intensity for all the centres was plotted as a function of the irradiation dose using Origin Pro 8 (Origin Lab Corporation, Northampton, USA). The dose response curves were obtained using an exponential linear function (Duval, 2012) and weighted the inverse of the squared ESR intensity ($1/I^2$) for each sample. De values were obtained by extrapolation.

No measurements could be performed in situ at the time of the excavation. External alpha, beta and gamma contributions were calculated from the radioelement contents (U, Th and K) measured in the sediment using a high resolution and low-background gamma-ray spectrometer and derived using the conversion factors of Guérin et al. (2011). A k-value of 0.15 ± 0.1 (Yokoyama et al., 1985; Laurent et al., 1998) and a water content of 15% (wet weight%) were used for calculation.

The alpha and beta attenuations factors are taken from Brennan et al. (1991) and Brennan (2003) respectively and the cosmic dose rate was calculated according to Prescott and Hutton (1994). The water attenuation factors follow Grün (1994). The internal dose rate was considered negligible due to the low radioelement content in quartz (Murray and Roberts, 1997; Vandenberghe et al., 2008).

Tab. 2. New samples collected for U-series (flowstone, tooth and bone), IRSL (feldspar), ESR/U-series (tooth) and ESR (quartz) analysed in this study. XJU: Xi'an Jiaotong University; LSCE: Laboratoire des Sciences du Climat et de l'Environnement; MNHN: Muséum national d'Histoire naturelle; SCU: Southern Cross University; VUW: Victoria University of Wellington.

Site	Sample type	Level	Depth (cm)	Sample #	Laboratory	Description
Payre	flowstone (U-Th)	H1a	320	18	XJU	-
		H2	400-500	19		-
		H3	400-500	20		-
		H4	400-500	21		-
		H5	400-500	22		-
		H6	400-500	23		-
		H7	400-500	24		-
Ranc Pointu	flowstone (U-Th)	top sequence	Residual flowstone	RCP1	LSCE	-
		top sequence	Top sequence	RCP2		-
		top sequence	Residual flowstone	RCP3		-
Abri du Maras	teeth (U-Th)	4.1	270	AM J6-111	SCU	*Rangifer Tarandus*
	bone (U-Th)	4.1	270	AM J6-116		fragment
Abri du Maras	feldspar (IRSL)	4.1	220	WLL922	VUW	-
		4.1	150	WLL923		-
		6	27	WLL924		-
Abri du Maras	teeth (ESR/U-series)	4.2	624	AM L11-412	MNHN	*Cervus elaphus*
		4.2	501	AM M10-369		*Bovidae*
Abri du Maras	soda straw (U-Th)	upper 5	536	AM L10-300	LSCE	-
		upper 5	394	AM M6-1199		-
		upper 5	437	AM L8-153		-
		upper 5	526	AM L10-307		-
		upper 5	456	AM M8-524		-
		upper 5	415	AM M6-1632		-
		upper 5	507	AM L10-170		-
		upper 5	398	AM N6-1001		-
		upper 5	412	AM 09-27		-
		upper 5	418	AM O9-23		-
		upper 5	516	AM M10-554		-
		upper 5	442	AM L8-249		-
		6	563	AM U10-503		-
		6	719	AM L13-46		-
		6	738	AM L14-5		-
		6	717	AM L13-45		-
		6	715	AM M12-74		-

Baume Flandin	bone (U-Th)	3	150	BF E7-33	SCU	fragment
Abri des Pêcheurs	tooth (U-Th)	D2	328	AP C8-01	SCU	*Rangifer Tarandus*
		D7	412	AP D5-84		*Rangifer Tarandus*
Le Figuier	tooth (ESR/U-series)	4 (room 2)	70	FIG-373	MNHN	*Capra ibex*
		4 (room 2)	70	FIG-405		*Bovinae*
Le Figuier	bone (U-Th)	6 (room 2)	60	FIG-24	SCU	fragment
	tooth (U-Th)	6 (room 3)	40	FIG-36		*Cervus*
Le Figuier	quartz (ESR)	1 (room 2)	220	FIG-1001	MNHN	-
		1 (room 2)	220	FIG-1002		-

3. Results

3.1. Payre

Uranium-series dating results obtained from the flowstone samples from Payre are presented in Table 3. Uranium content is low for all samples, ranging from 123 to 516 ppb. We observe the highest U-content in the samples taken from the oldest part of the flowstone. Samples #23 and #24, coming from the base of the flowstone, have a U-content of 435 and 516 ppb respectively, whereas samples #18 to #22, which come from the middle and top of the formation, show a U-content ranging from 123 to 223 ppb. ^{232}Th content ranges from 12 to 106 ppb and the ^{230}Th/^{232}Th ratio, which was measured to control detritic contamination, ranges from 39 ± 1 to 226 ± 5. Uncorrected and corrected ages thus do not significantly differ. When considering the error range, corrected ages fall within the range of uncorrected ages, except for sample #18. An age difference of 10 ka is observed between the mean corrected and uncorrected ages. However, the seven ages obtained from the flowstone do not follow the stratigraphic order. Those obtained for the base of the flowstone, H6 (sample #23) and H7 (sample #24) are 114802 ± 4241 years and 128632 ± 2532 years, respectively. Ages obtained from the middle part of the flowstone, H3, H4 and H5 (samples #20, #21 and #22) are 268427 ± 4377 years, 266329 ± 5409 years and 283282 ± 3770 years, respectively, and are thus older than those from the base of the flowstone. The upper levels of the flowstone, H1 and H2, provided ages of 178221 ± 7468 years and 331121 ± 6880 years, respectively. Fig. 5a presents the ^{238}U and ^{232}Th content as well as the corrected ages for the Payre samples. The highest U-contents are correlated with younger ages at the base of the flowstone (samples #23e24, which are the oldest considering their stratigraphic position), and the lowest U-content with the oldest ages (samples #19-22, from the youngest part of the flowstone). Only sample #18, from the top of the flowstone, does not seem affected by this trend. The ^{232}Th content is not correlated to the age nor the U-content. Fig. 5b plots the U-content as a function of the ^{230}Th/^{234}U ratios. We can observe an

inverse relation between ages and U-content. A similar feature was observed at Nerja Cave in Spain (Pons-Branchu et al., 2020) and interpreted as a possible loss of uranium in some of the samples. U-leaching in some of the samples led to an increase in the ^{230}Th/^{234}U values and provided overestimated apparent ages. According to these data, the stratigraphic inversion observed does not seem linked to contamination from ^{232}Th, but it is likely due to diagenetic processes that led to U mobility, especially in the middle and upper part of the flowstone. Taking into account these observations, the ages obtained should be considered with caution as a terminus post quem for the overlying sequence.

3.2. Ranc-Pointu 2

Uranium-series ages obtained from the three flowstone samples are presented in Table 3. U-content is low, ranging from 270 to 331 ppb. ^{230}Th/^{232}Th ratios are low in samples RCP2 and RCP3, 4 ± 1 and 12 ± 1, respectively. Corresponding corrected ages are 109735 ± 8531 years (uncorrected is 125303 ± 1416 years) and 85138 ± 2714 years (uncorrected is 89321 ± 699 years). In sample RCP1, ^{230}Th/^{232}Th is 659 ± 3, uncorrected and corrected are thus not distinguishable (56732 ± 426 and 56677 ± 453 respectively). RCP2 gives a minimum age estimate for the overlying archaeological layer c, ca. 110 ka, and it likely precipitated during MIS 5d. RCP1 and 3 cannot be directly related to the stratigraphy because they are remnants of flowstones. However, they give information about karst activity, and suggest that climatic conditions were favourable for the precipitation of speleothems during MIS 5a/b (RCP3, ca. 85 ka) and at the beginning of MIS 3 (RCP1, ca. 57 ka).

3.3. Baume Flandin

Three U-series analyses were conducted on the bone from Baume Flandin (layer 3) and the results are presented in Table 3. BF-U is the upper sample (closest to the outer surface of the bone), BF-M is the middle sample (half way between the outer surface and the centre of the bone), BF-L is the lower sample (in the centre of the bone) (Fig. 6). Corrected ages range from 108776 ± 2071 to 116827 ± 1543 years. U-content is homogeneous among the sub-samples, ranging from 16.3 ± 0.01 to 20.1 ± 0.01 ppm. ^{230}Th/^{232}Th ratios are low, ranging from 13 ± 0.1 to 20 ± 0.1 and indicating contamination from exogeneous Th, likely due to the porous nature of the samples. Uncorrected ages range from 113168 ± 476 to 119279 ± 686 ka, and both corrected and uncorrected ages fall within MIS 5. As expected, the isotopic signature of these three subsamples is homogeneous, with δ^{234}U ranging from 52.6 ± 1.0 to 58.5 ± 1.1 and ^{230}Th/^{234}U ratios ranging from 0.6842 ± 0.0015 to 0.7115 ± 0.0022. According to these ages, layer 3 can be attributed to the beginning of MIS 5.

3.4. Abri du Maras

Uranium-series ages obtained on the soda straws (layers upper 5 and 6) and the bones and teeth (layer 4.1) are presented in Table 3. U-content in the soda straws ranges from ca. 1358 to 2249 ppb except for one sample that contains 3457 ppb of U (AM L8-153). This sample also provides the lowest ^{230}Th/^{238}U ratio (0.8669 ± 0.0025). Indeed, for 12 out of the 17 dated samples, ^{230}Th/^{238}U ratios are higher than 1, and for 10 of them, secular equilibrium has been reached thus precluding age calculation. Seven samples provided corrected ages ranging from 207 ± 3 to 497 ± 48 ka. ^{230}Th/^{232}Th are higher than 75, indicating a low contamination from exogenous thorium. Fig. 7 plots the U-content as a function of the ^{230}Th/^{234}U ratios. As for the samples from Payre, we can observe an inverse correlation between ages and U-content that may indicate uranium leaching. Indeed, the ages obtained are much older than the age of layer upper 5 by ESR/U-series of 90 ± 9 ka (Richard et al., 2015, Table 1). These results could be interpreted in two ways: i) the stalactites grew during an earlier and more suitable period for speleothem formation between MIS 14 or 10 and broke only thousands of years later and were incorporated in layer dated to MIS 5 (for layer upper 5) or earlier (layer 6); ii) the stalactites found in layer upper 5 are contemporary with MIS 5 as suggested by the ESR/U-series age but underwent diagenesis and U-loss during burial (a similar scenario may apply to the samples from layer 6 for which no other dates are available).

The observation of four soda straw samples (16e35 mm long and 5e10 mm in diameter) from levels upper 5 and 6 using a binocular microscope (SOM Fig. S6) gave some insights to interpret these dates. The results indicate that: (i) the breaks are never straightforward and are, on the contrary, quite rounded, (ii) no central canal could be recognised, (iii) surface alteration is visible (small etching pit), also affecting the breaks and finally (iv) no heliotropic growths are visible. These preliminary elements show that the stalactite fragments must have been of greater length before they broke. They have undergone, most certainly in the sediment, a post-breakage alteration affecting both the breaks and the periphery. Finally, the absence of heliotropic excrescence suggests that the growth of these samples took place in a dark context. These samples, sealed in levels upper 5 and 6, are therefore important markers for reconstructing the paleo-geometry of the rock shelter before the ceiling collapsed. These observations support the hypothesis according to which the UeTh ages of the soda straws are much older than the layer in which they were buried. Indeed, the fact that they precipitated while the site was closed (absence of sunlight) may be compatible with an early chronology, i.e., MIS 14e10 as suggested by the ages obtained. However, considering the possible issues related to uranium leaching and that the precipitation of the speleothems occurred before their burial, these ages represent a terminus post quem for the levels where they were uncovered.

On the contrary, U-series dating of bones and teeth is generally considered as minimum age estimates, because the time span between the burial and the uranium uptake is unknown. That is the reason why ESR is generally

combined with U-series to date dental remains. Moreover, it is reasonable to consider that bones can also suffer from U leaching, as it was demonstrated in a number of studies (e.g., Millard and Hedges,1995; Sambridge et al., 2012; Grün et al., 2014). In this study, one tooth (AM J6-111, a large reindeer pre-molar) and one connected bone (AM J6-116, most likely a phalange from a bovid or cervid) were dated. They provided uncorrected ages of 57766 ± 316 and 16907 ± 131 years and corrected ages of 56738 ± 580 and 3150 ± 7331 years respectively. The tooth showed minimal alteration, in fact roots and enamel were intact. It had very light discoloration from cream to light brown and no apparent cracks. On the other hand, the bone was heavily weathered, with a large amount of clay that may have contaminated it. For the latter, the U-content is low (~1 ppm) while in the tooth it is much higher (~25 ppm). High U-content in bones and dental tissues such as dentine or cement is generally observed because they are porous (the mineral phase, carbonate hydroxyapatite, represents only 60-70%, Lees, 1987). Moreover, the $^{230}Th/^{232}Th$ of the bone is ~1 (against ~36 in the tooth), indicating significant contamination by ^{232}Th, likely from the clay attached to the sample. Considering the above, the sample does not fulfil the conditions required to provide a reliable age, even a minimum one, thus the age obtained should be discarded. The age obtained for the tooth, of 57 ± 1 ka, is slightly older than those previously obtained for layers 4.1 and 4.2, ranging from 40 ± 3 to 55 ± 5 ka (Richard et al., 2015). Due to the nature of the sample, U-leaching cannot be excluded and could explain this age difference.

ESR/U-series ages obtained on two teeth sampled in level 4.2 are presented in Table 4. Equivalent doses (De) are 80 ± 2 and 67 ± 1 Gy for samples AM L11e412 and AM M10-369, respectively (SOM Fig. S7), and are in the same range as those obtained for samples from layers 4.1 and 4.2 previously published (Richard et al., 2015, see synthesis in SOM Table S2). The dose rate was measured in situ (633 $\mu Gy.a^{-1}$) and falls within the variability of the gamma dose measured at the site (ranging from ~422 to 915 $\mu Gy \cdot a^{-1}$, Richard et al., 2015), typical of heterogeneous deposits made of aeolian silts and limestone blocks (corresponding to the roof collapse). U, Th and K contents measured using laboratory gamma-ray spectrometry are presented in SOM Table S3. Radioelement content is similar in the two samples and the corresponding beta dose rates are low, 104 ± 14 and 48 ± 8 $\mu Gy \cdot a^{-1}$ for AM L11e412 and AM M10-369, respectively. The high U content in the dentine (from ~88 to 97 ppm, Table 3) provides a beta dose rate of 622 ± 245 (AM M10-369) and 946 ± 101 $\mu Gy \cdot a^{-1}$ (AM L11-412), which represents up to 50% of the total dose rate for AM L11-412. As expected for the enamel, the U-content is significantly lower, ranging from ~0.73 to 2.16 ppm (Table 3), as is the internal dose rate (140 ± 17, AM L11-412 and 229 ± 79 $\mu Gy \cdot a^{-1}$, AM M10-369). The U-series model proposed by Grün et al. (1988) allows the reconstruction of the U-uptake history and the corresponding dose rate in the dental tissue by calculating the U-uptake parameter, the 'p-value', ranging from 1 (describing an early uptake, EU, which occurred soon after burial) to positive values (describing a recent uptake). The model takes into account isotopic ratios in both enamel and dentine

(^{234}U/^{238}U and ^{230}Th/^{234}U). However, the application of the model is limited to samples that did not undergo U leaching. For the Maras teeth, the model can be applied only to AM M10-369, for which an age of 42 ± 6 ka was obtained. For AM L11-412, U-leaching was detected in the dentine. The U-series age of the dentine, of 47 ka, is slightly older than the EU age calculated. The EU age, of 42 ± 3 ka, can thus be used as a minimum age.

IRSL ages are presented in Table 5. Equivalent doses for layer 4.1 are 111 ± 7 and 199 ± 6 Gy and the dose rates are 2416 ± 110 and 3180 ± 132 μGy·a-1. Although these two samples were taken from the same level, the high heterogeneity of the deposits composed of various limestone blocks is reflected in the De and dose rate values that differ greatly from one sample to the other. Moreover, no in-situ dosimetry could be performed where the samples were taken and the dose rate may be inaccurate. This could explain the age difference between these two samples, 46 ± 4 ka (WLL 922) and 63 ± 3 ka (WLL 923). However, the age of 46 ± 3 ka is in agreement with previous (Richard et al., 2015) and new ESR/U-series data (Table 4) obtained for layers 4.1 and 4.2. It is possible that some grains were not fully bleached before deposition for WLL 923, thus overestimating the equivalent dose. The age of 51 ± 3 ka (WLL 924) obtained for layer 6 falls within the same range than the ages obtained for layers 4.1 and 4.2 and is younger than previous ages obtained for layer 5-upper 5, ranging from ~91 to 72 ka (Moncel et Michel, 2000; Richard et al., 2015, see Table 1). Like for the other two samples, no in-situ dosimetry can be performed for this layer. An overestimation of the dose rate, which was derived from a sediment sample and thus may not take into account the presence of large limestone blocks in the surrounding of the sample, cannot be excluded and would lead to an underestimation of the age for layer 6.

3.5. Abri des Pêcheurs

The U-series results obtained for the two teeth from Abri des Pêcheurs are presented in Table 3. U-content is heterogeneous among the samples, ranging from ~1.8 (AP C8-01) to ~6.9 ppm (AP D5-84). ^{230}Th/^{232}Th ratios are 2 and 3, indicating exogeneous contamination. Indeed, uncorrected and corrected ages vary greatly and are, respectively, 41176 ± 475 and 23357 ± 9344 years for AP C8-01 and 29393 ± 211 and 22390 ± 3488 years for AP D5-84. Considering the above, these ages must be used with caution, due to the uncertainty related to both contamination in exogeneous thorium and uranium uptake that greatly affect the age calculation.

3.6. Grotte du Figuier

Two U-series ages were obtained for rooms 2 and 3 on a bone and a tooth. As for Pêcheurs samples,

detritic contamination is significant (^{230}Th/^{232}Th 6). The U-content ranges from ~15 to 18 ppm and d^{234}U values are negative. ^{234}U/^{238}U < 1 were also measured in a tooth from room 1 (Richard et al., 2015) and in the teeth dated by ESR/U-series in this study (Table 3), and indicate that

these ratios are depleted in ^{234}U, likely due to the weathering of rocks or soils, as observed in speleothems from Chauvet Cave, located at 20 km from the Figuier cave (Genty et al., 2004). Corrected ages obtained are 33670 ± 6618 years (45738 ± 250 years uncorrected) and 12520 ± 922 ka (14303 ± 96 years uncorrected) for samples FIG-24 (room 2) and FIG-36 (room 3), respectively. Considering that they were recovered in a Middle Palaeolithic context, the age of the samples should be considered as a minimum age estimate.

ESR/U-series ages obtained from two teeth are presented in Table 4. Equivalent doses range from 51 ± 2 and 65 ± 1 Gy. Dose response curves are shown in SOM Fig. S7. The U content of the dentine ranges from ~17 to 22 ppm and is lower in the enamel, ~0.14-0.27 ppm (Table 3). Corresponding dose rates are low (<327 µGy.a—1) and the main contribution to the dose rate is from the sediment, with values ~1565e1578 µGy.a—1. Ages obtained for level 4 are 29 ± 4 ka (FIG-373) and 40 ± 4 ka (FIG-405), suggesting a deposition during MIS 3. However, there is a discrepancy of 10 ka between these two ages. Considering that the measured gamma dose contributes to more than 60% of the dose rate for the two samples and that they show a similar dose rate distribution (Fig. 8), the difference lies in the two distinct De, of 51 ± 2 Gy (FIG-373) and 65 ± 1 Gy (FIG-405). These could be related to dosimetric heterogeneity in the dated layer or to possible reworking. For the latter, the present-day dose rate would not be representative of the past one, thus giving an erroneous age. Indeed, coprolites, bear and hyena cubs were documented in rooms 2 and 3, suggesting the occupation of the cave as a den by carnivores (Moncel et al., 2012b). Disturbance of the human occupation layers due to carnivore activity cannot be excluded and would explain the age discrepancy observed in layer 4.

ESR dating on quartz samples from room 2 (layer 1, base) provided Middle Pleistocene ages (1s) spanning from 185 ± 90 ka (Fig. 1002) to 335 ± 39 ka (Fig. 1001) considering the Al centre, and from 305 ± 36 ka (Fig. 1002) to 378 ± 30 ka (Fig. 1001) considering the Ti-Li centre (Table 6 and SOM Fig. S8). Bleaching rates for the Al centre are 39% (Fig. 1001) and 55% (Fig. 1002). For the Ti-Li centre, they reach 100% for both samples (Table 6). For Fig. 1001, Al and Ti-Li ages, of 335 ± 39 ka and 378 ± 30 ka respectively, are consistent at $\pm$ 1 s, which is acceptable for the Multiple Centre (MC) approach. A moderate goodness of fit value was obtained for the Al centre, with a coefficient of determination (r^2) of 0.986 while a r^2 of 0.997 was obtained for the Ti centre, considered as an excellent goodness of fit (Duval and Guilarte, 2015). For Fig. 1002, ages obtained from the Al and Ti-Li centres do not respect the MC approach (185 ± 90 ka and 305 ± 36 ka, respectively). While the Ti-Li centre provides r^2 of 0.993 (excellent goodness of fit value) and an age of 305 ± 36 ka, similar to those obtained from Fig. 1001, the Al centre yields r^2 of 0.985 (moderate goodness of fit value) and a low D_e (278 ± 134 Gy) giving an age estimate of 185 ± 90 ka, which is not in agreement with all

other available ages. The high error on the Al centre De may be due to the instability of the ESR spectrometer during measurements (moderate goodness of fit values, Duval, 2012). High standard deviations were obtained for the ESR intensities of the low doses (first points of the DRC, SOM Fig. S8). The Al age for FIG1002 should be thus used with caution. For both samples, the Ti-Li centre is considered to be more reliable, considering the consistency between the two samples in the same layer and with the Al age of Fig. 1001. Moreover, the optical bleaching difference suggests a potential variability of the quartz grains, which should be considered carefully as cave fluvial sediments often happen to be mixed with more ancient ones, thus revealing complex burial histories (Sadier, 2013; Tassy et al., 2013; Harmand et al., 2017; Sartégou et al., 2018). Here, despite the absence of in-situ gamma measurements, the values of the dose rate for both samples (1437 ± 22 for Fig. 1001 and 1480 ± 45 for Fig. 1002, Table 6) are similar with comparable U, Th and K contents measured in both samples (see details in SOM Table S3). The dose rate values are similar to those obtained on other Ardèche river fluvial deposits (see Genuite et al., 2021). Ages obtained for Fig. 1001 (Al and Ti-Li centres) and Fig. 1002 (Ti-Li centre) are consistent and indicate a deposition of layer 1 during the Middle Pleistocene, between MIS 11 and 8.

Tab. 3. U-series results (2σ). Ages were calculated using the following U decay constants: l238 = 1.55125 × 10^{-10} (Jaffey et al., 1971) and l234 = 2.82206 × 10^{-6} (Cheng et al., 2013) and Th decay constant: l230 = 9.1705 × 10^{-6} (Cheng et al., 2013). δ^{234}U = ([^{234}U/^{238}U]$_{activity}$ − 1) × 1000. δ^{234}U$_{initial}$ was calculated based on ^{230}Th age (T), i.e., δ^{234}U$_{initial}$ = δ^{234}U$_{measured}$× e^{l234xT}. Corrected ^{230}Th ages assume the initial ^{230}Th/^{232}Th atomic ratio of 4.4 ± 2.2 × 10^{-6}. Those are the values for a material at secular equilibrium, with the bulk earth ^{232}Th/^{238}U value of 3.8. The errors are arbitrarily assumed to be 50%.

Abbreviations: n.d. = not detectable; F = flowstone; E = enamel; D = dentine; S = soda straw; B = bone; T = tooth.

[a]The U-series data obtained on these dental tissues were combined with ESR data to model the U-uptake (see text).

[b]Dates are reported as ka Before Present (BP), where the Present stands for the year 1950 CE.

Site	Sample type	Lab #	Sample #	^{238}U(ppb)	^{232}Th (ppb)	^{230}Th/^{232}Th	δ^{234}U	^{230}Th/^{238}U	Age (ka)	Corr. age (ka)	Corr. age (ka BP)[b]	δ^{234}U$_{Initial}$
Payre	F	18	H1	223.3 ± 0.4	87.86 ± 1.76	39 ± 1	99.2 ± 2.1	0.9225 ± 0.0023	188.506 ± 1.663	178.221 ± 7.468	178.154 ± 7.468	164 ± 5
	F	19	H2	123.4 ± 0.2	17.69 ± 0.35	120 ± 2	68.5 ± 1.8	1.0407 ± 0.0023	334.730 ± 6.605	331.121 ± 6.880	331.054 ± 6.880	174 ± 8
	F	20	H3	147.2 ± 0.2	23.99 ± 0.48	100 ± 2	62.7 ± 1.8	0.9925 ± 0.0018	272.692 ± 3.304	268.427 ± 4.377	268.360 ± 4.377	134 ± 9
	F	21	H4	206.0 ± 0.3	50.15 ± 1.01	68 ± 1	69.9 ± 1.8	1.0010 ± 0.0018	272.673 ± 3.195	266.329 ± 5.409	266.262 ± 5.409	148 ± 4
	F	22	H5	159.2 ± 0.2	11.55 ± 0.23	226 ± 5	57.2 ± 1.7	0.9960 ± 0.0017	285.171 ± 3.591	283.282 ± 3.770	283.215 ± 3.770	127 ± 4
	F	23	H6	434.5 ± 0.6	105.30 ± 2.11	54 ± 1	159.6 ± 1.8	0.7929 ± 0.0018	120.728 ± 0.607	114.802 ± 4.241	114.735 ± 4.241	221 ± 2
	F	24	H7	516.0 ± 0.1	72.44 ± 1.46	97 ± 2	148.7 ± 2.0	0.8240 ± 0.0020	132.049 ± 0.776	128.632 ± 2.532	128.565 ± 2.532	214 ± 4
Ranc Pointu	F	5398	RCP1	270.19 ± 0.1	0.412 ± 0.01	659 ± 3	-167.0 ± 1.0	0.3323 ± 0.0014	56.732 ± 0.426	56.677 ± 0.453	54.612 ± 0.453	-196.0 ± 1.2
	F	5399	RCP2	281.25 ± 0.1	156.07 ± 0.14	4 ± 1	-41.8 ± 1.6	0.6494 ± 0.0026	125.303 ± 1.416	109.735 ± 8.531	109.504 ± 8.531	-59.5 ± 2.3
	F	5400	RCP3	331.06 ± 0.1	43.97 ± 0.04	12 ± 1	-85.4 ± 1.3	0.5053 ± 0.0017	89.321 ± 0.699	85.138 ± 2.714	83.107 ± 2.714	-109.9 ± 1.7
Abri du Maras	E	ICP190 07_6	AM L11-412[a]	725.7 ± 30.4	1.583 ± 0.07	368 ± 8	78.0 ± 41.7	0.2630 ± 0.0110	-	-	-	-
	D	ICP190 07_1	AM L11-412d[a]	96730.4 ± 4230.7	6.542 ± 0.30	17051 ± 360	80.6 ± 43.1	0.3773 ± 0.0160	-	-	-	-
	E	ICP190 07_7	AM-M10-369[a]	2163.7 ± 91.5	5.930 ± 0.26	245 ± 5	73.4 ± 42.3	0.2194 ± 0.0094	-	-	-	-
	D	ICP190	AM M10-	88343.3 ±	2.780 ±	26675 ±	47.5 ±	0.2747	-	-	-	-

Site	Type	Lab code	Sample									
		07_2	369[a]	3772.5	0.13	560	42.4	± 0.0115				
	S	8612	AM L10-300	2113.4 ± 17.6	59.42 ± 0.77	122 ± 1	12.0 ± 0.7	1.0637 ± 0.0113	sup 500	sup 500	sup 500	n.d.
	S	8601	AM M6-1199	1847.1 ± 15.7	19.53 ± 0.17	297 ± 1	13.5 ± 1.0	1.0269 ± 0.0036	sup 500	sup 500	sup 500	n.d.
	S	8602	AM L8-153	3456.7 ± 30.3	60.21 ± 0.51	153 ± 1	15.0 ± 1.1	0.8669 ± 0.0025	207.922 ± 2.646	207.386 ± 2.902	207.316 ± 2.903	26.9 ± 2.1
	S	8603	AM L10-307	1924.9 ± 15.9	26.94 ± 0.22	215 ± 1	9.7 ± 1.0	0.9810 ± 0.0022	377.353 ± 11.891	376.938 ± 12.062	376.868 ± 12.063	28.1 ± 3.1
	S	8606	AM M8-524	2151.0 ± 17.5	52.63 ± 0.44	124 ± 1	16.5 ± 1.5	0.9876 ± 0.0026	370.394 ± 13.909	369.689 ± 14.187	369.619 ± 14.188	46.8 ± 4.6
	S	8613	AM M6-1632	2202.0 ± 17.9	30.87 ± 0.31	228 ± 1	16.7 ± 0.6	1.0425 ± 0.0061	sup 500	sup 500	sup 500	n.d.
	S	8614	AM L10-170	2233.3 ± 18.1	58.94 ± 0.50	125 ± 1	19.1 ± 0.7	1.0713 ± 0.0032	sup 500	sup 500	sup 500	n.d.
	S	8615	AM N6-1001	1701.5 ± 13.7	16.12 ± 0.14	322 ± 1	16.6 ± 1.2	0.9932 ± 0.0029	388.968 ± 16.461	388.697 ± 16.563	388.627 ± 16.564	49.7 ± 4.3
	S	8599b	AM 09-27	1357.9 ± 11.0	42.90 ± 0.39	104 ± 1	4.1 ± 1.3	1.0731 ± 0.0044	sup 500	sup 500	sup 500	n.d.
	S	8617	AM O9-23	1729.1 ± 14.0	25.98 ± 0.22	205 ± 1	13.1 ± 1.1	1.0066 ± 0.0036	497.747 ± 47.955	497.347 ± 47.999	497.277 ± 47.100	53.4 ± 8.4
	S	8619	AM M10-554	1812.1 ± 14.6	27.88 ± 0.24	200 ± 1	20.0 ± 0.8	1.0079 ± 0.0031	434.011 ± 23.040	433.585 ± 23.179	433.515 ± 23.180	68.2 ± 5.3
	S	8620	AM L8-249	1920.3 ± 15.6	54.37 ± 0.46	133 ± 1	6.4 ± 1.1	1.2310 ± 0.0039	sup 500	sup 500	sup 501	n.d.
	S	8600	AM U10-503	1652.0 ± 13.8	13.97 ± 0.12	360 ± 2	9.7 ± 0.8	0.9926 ± 0.0049	429.154 ± 31.924	428.918 ± 31.982	428.848 ± 31.983	32.6 ± 4.0
	S	8604	AM L13-46	1539.4 ± 12.4	65.87 ± 0.54	75 ± 1	24.3 ± 1.0	1.0397 ± 0.0021	sup 500	sup 500	sup 500	n.d.
	S	8616	AM L14-05	1830.7 ± 14.8	35.02 ± 0.32	165 ± 1	16.6 ± 1.1	1.0319 ± 0.0043	sup 500	sup 500	sup 500	n.d.
	S	8618	AM L13-45	1776.5 ± 14.3	16.90 ± 0.15	324 ± 1	2.1 ± 1.4	1.0063 ± 0.0038	sup 500	sup 500	sup 500	n.d.
	S	8621	AM M12-74	2248.8 ± 18.1	24.69 ± 0.21	284 ± 1	8.1 ± 1.4	1.0197 ± 0.0033	sup 500	sup 500	sup 500	n.d.
Abri du Maras	T	ADM-SCU-03-US	AM J6-111	25187.5 ± 15.0	951.70 ± 2.84	35.9 ± 0.2	81.9 ± 1.1	0.4471 ± 0.0018	57.766 ± 0.316	56.738 ± 0.580	56.677 ± 0.580	97.2 ± 1.4
	B	ADM-SCU-04-US	AM J6-116	984.6 ± 0.4	440.80 ± 2.71	1 ± 0.1	27.9 ± 1.4	0.1475 ± 0.0010	16.907 ± 0.131	3.150 ± 7.331	3.089 ± 7.331	32.0 ± 2.7
Baume Flandin	B	BF-SCU06	BFE7-33	2011.4 ± 8.4	2225.02 ± 12.43	19.5 ± 0.1	58.5 ± 1.1	0.7115 ± 0.0022	119.279 ± 0.686	116.827 ± 1.543	116.766 ± 1.543	83.9 ± 2.0

	B	BF-SCU06-M	BF E7-33	1690.2 ± 7.2	2626.79 ± 9.62	13.4 ± 0.1	52.6 ± 1.0	0.6842 ± 0.0015	113.168 ± 0.476	108.776 ± 2.071	108.715 ± 2.071	74.8 ± 2.0
	B	BF-SCU06-L	BF E7-33	1629.8 ± 8.7	2189.63 ± 8.02	16.0 ± 0.1	55.0 ± 0.9	0.7067 ± 0.0021	113.907 ± 0.710	115.509 ± 1.831	115.448 ± 1.831	79.1 ± 1.9
Abri des Pêcheurs	T	ADP-SCU02	AP C8-01	1797.9 ± 9.0	1143.8 ± 3.80	1.7 ± 0.1	136.1 ± 1.4	0.3593 ± 0.0034	41.176 ± 0.475	23.357 ± 9.344	23.296 ± 9.344	175.8 ± 16.1
	B	ADP-SCU03	AP D5-84	6866.8 ± 2.8	1833.7 ± 11.20	3.1 ± 0.1	156.7 ± 1.0	0.2745 ± 0.0017	29.393 ± 0.211	22.390 ± 3.488	22.329 ± 3.488	180.3 ± 6.2
Grotte du Figuier	E	5899	FIG-373[a]	266.7 ± 0.9	1.72 ± 0.01	79.5 ± 6	-104.6 ± 11.8	0.1714 ± 0.0116	-	-	-	-
	D	5901	FIG-373[a]	16691.2 ± 94.9	1.89 ± 0.02	3735.5 ± 84	-137.7 ± 4.4	0.1413 ± 0.0028	-	-	-	-
	E	5900	FIG-405[a]	142.3 ± 0.5	0.62 ± 0.01	46.2 ± 8	-251.6 ± 17.0	0.0672 ± 0.0110	-	-	-	-
	D	5902	FIG-405[a]	21810.9 ± 168.0	3.51 ± 0.04	1229.7 ± 31	-294.4 ± 3.8	0.0662 ± 0.0015	-	-	-	-
	B	GDF-SCU04	FIG-24	1465.0 ± 5.6	5063.1 ± 23.00	2.7 ± 0.1	-91.0 ± 1.0	0.3091 ± 0.0013	45.738 ± 0.250	33.670 ± 6.618	33.609 ± 6.618	-110.5 ± 7.0
	T	GDF-SCU05	FIG-36	1818.1 ± 8.0	893.3 ± 2.30	6.3± 0.1	-168.1 ± 0.8	0.1017 ± 0.0060	14.303 ± 0.096	12.520 ± 0.922	12.459 ± 0.922	-176.6 ± 1.8
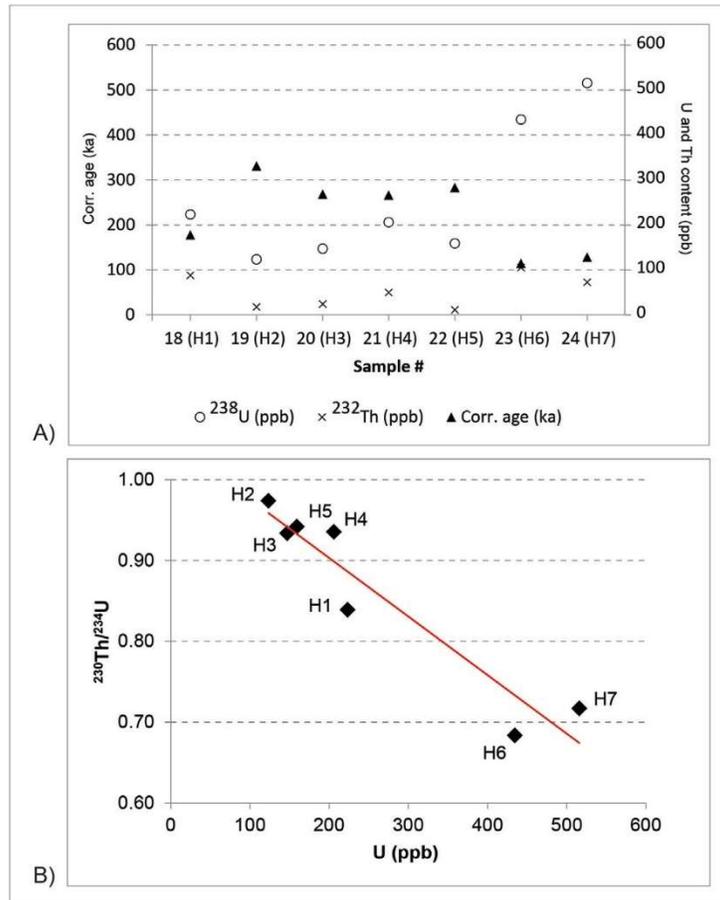
Fig. 5. Payre. Graphic representation of U-series data. A) U and Th contents, and corrected ages of the samples. B) U content versus ^{230}Th/^{234}U ratios.
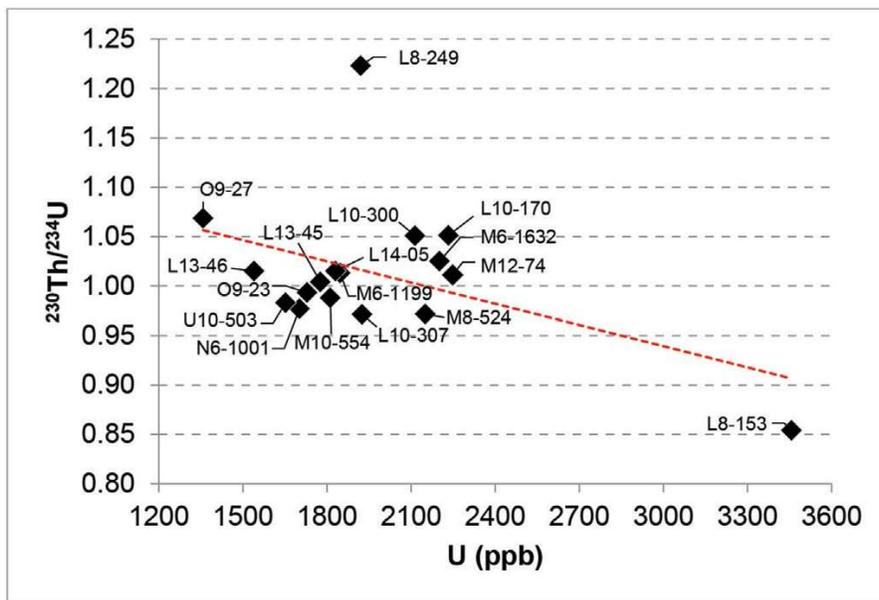
Fig. 7. Abri du Maras. Graphic representation of U-content plotted as a function of ^{230}Th/^{234}U ratios.

A

B

~117 ka

~109 ka

~116 ka

U/Ca

U (ppm)

20

15

10

0   1   2   3

Distance from center (cm)

Laser track

BF-L

BF-M

BF-U

BF-U upper sample (closest to outside of the bone), BF-M middle sample, BF-L lower sample (in the centre of the trabecular bone)

Sample	U (ppm)	$^{230}Th/^{232}Th$	$^{230}Th/^{238}U$	$^{234}U/^{238}U$	Corr. Int. $^{234}U/^{238}U$	Corrected ages
BF-U	20.1140 +/- 0.01	19.52	0.7115+/- 0.0022	1.0585+/- 0.0012	1.0839+/- 0.0021	**116.8 +/-1.5**
BF-M	16.9020 +/- 0.01	13.36	0.6842+/- 0.0015	1.0526+/- 0.0010	1.0748+/- 0.0022	**108.8 +/-2.1**
BF-L	16.2976 +/- 0.01	15.96	0.7067+/- 0.0021	1.0550+/- 0.0010	1.0791+/- 0.0021	**115.5 +/-1.8**

Fig. 6. Baume Flandin. Sampling positions (A) and U-series results (B) obtained on the bone.

Tab. 4. ESR/U-series results (1σ) obtained on enamel hydroxyapatite from Abri du Maras and Grotte du Figuier (room 2). The water content is expressed in wet weight %. The age were modeled using either the Early Uptake (EU) or the U-series (US) models (see text).

Site	Level	Sample #	D_e (Gy)	Water content (%)	Dose rate (μGy/a)				Uptake parameter (p or n)		Age (ka)	Model
					sediment (β + γ) + cosmic	internal (α + β)	dentine (β)	total	enamel	dentine		
Abri du Maras	4.2	AM L11-412	80 ± 2	15	794 ± 66	140 ± 17	946 ± 101	1880 ± 122	-1	-1	42 ± 3	EU
	4.2	AM M10-369	67 ± 1	15	751 ± 64	229 ± 79	622 ± 245	1602 ± 265	-0.36 ± 0.25	-0.76 ± 0.20	42 ± 6	US
Grotte du Figuier	4	FIG-373	51 ± 2	10	1578 ± 137	34 ± 42	147 ± 180	1759 ± 230	-0.77 ± 0.12	-0.55 ± 0.14	29 ± 4	US
	4	FIG-405	65 ± 1	10	1565 ± 137	5 ± 5	55 ± 59	1625 ± 149	1.78 ± 0.19	1.60 ± 0.18	40 ± 4	US

Tab. 5. IRSL results (1σ) obtained on the sediment samples from Abri du Maras. U, Th and K content was used to derive the dose rate (see details in SOM Tab. S3). The water content is expressed in water/dry mass of sediment %.

Level	Sample #	D_e (Gy)	a-value	Water content (%)	Dose rate (μGy/a)			Age (ka)
					sediment ($\alpha + \beta + \gamma$)	cosmic	total	
4.1	WLL922	111 ± 7	0.09 ± 0.01	16	2346 ± 110	70 ± 4	2416 ± 110	46 ± 4
4.1	WLL923	199 ± 6	0.07 ± 0.01	14	3105 ± 132	75 ± 4	3180 ± 132	63 ± 3
6	WLL924	130 ± 4	0.07 ± 0.01	22	2508 ± 109	60 ± 3	2568 ± 109	51 ± 3

Tab. 6. ESR results (1σ) obtained on quartz samples from Grotte du Figuier (layer 1, room 2). Al: data obtained from the Aluminium centre; Ti-Li: data obtained from the Titanium-Lithium centre; δbl (%) is the optical bleaching rate of quartz grains; r^2 is the coefficient of determination and express the quality of the fitting of the dose response curve. The water content is expressed in wet weight %.

Sample #	D_e (Gy)	δbl (%)	r^2	Water content (%)	Dose rate (μGy/a)			Age (ka)
					Sediment ($\alpha + \beta + \gamma$)	Cosmic	Total	
Fig 1001 Al	488 ± 56	39	0.986	15	1437 ± 22	19 ± 1	1456 ± 22	335 ± 39
Fig 1001 Ti-Li	550 ± 43	100	0.997	15	1437 ± 22	19 ± 1	1456 ± 22	378 ± 30
Fig 1002 Al	278 ± 134	55	0.985	15	1480 ± 45	19 ± 1	1499 ± 45	185 ± 90
Fig 1002 Ti-Li	457 ± 52	100	0.993	15	1480 ± 45	19 ± 1	1499 ± 45	305 ± 36
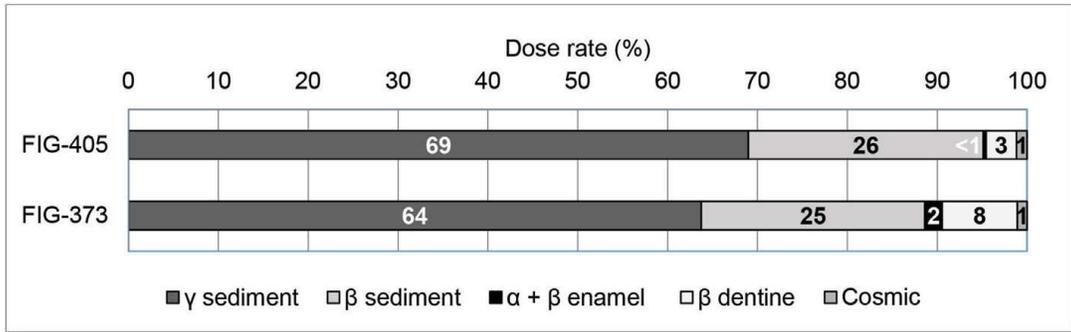
Fig. 8. Grotte du Figuier. Dose rate distribution (%).
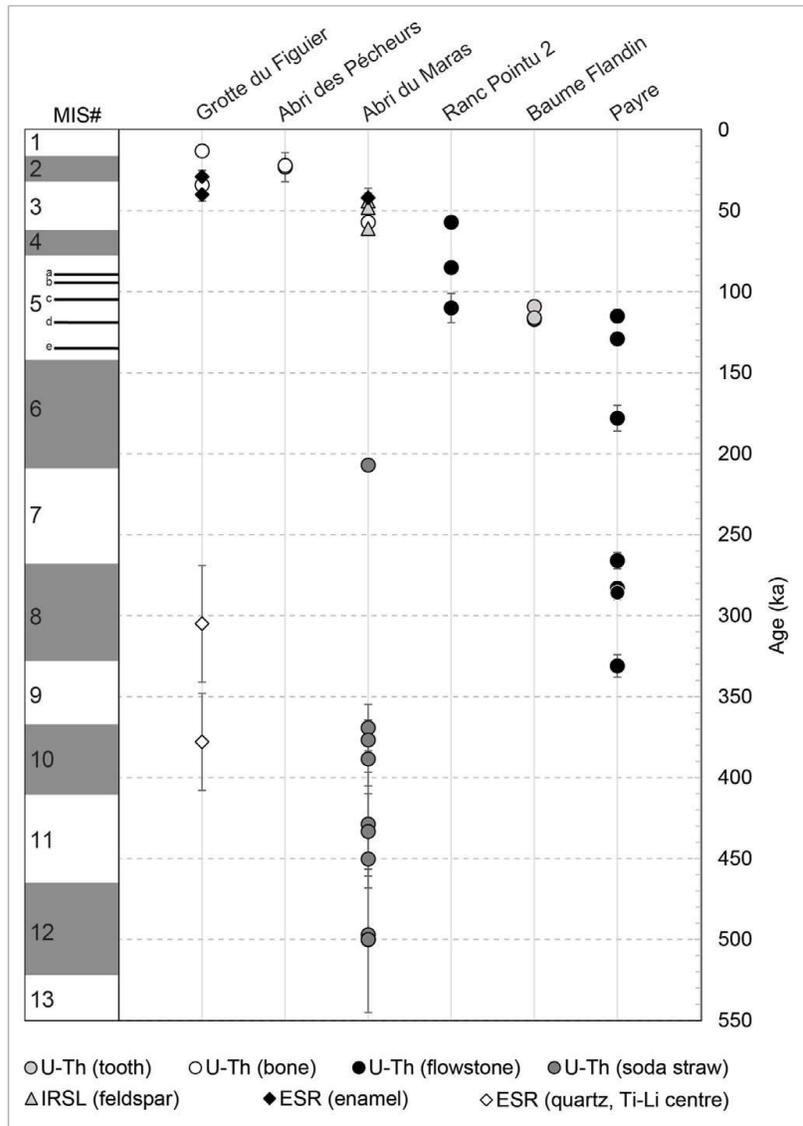
Fig. 9. Graphic representation of the ages obtained in this study as a function of marine isotopic stages. For some of the U-series ages, error bars are not visible due to the scale.
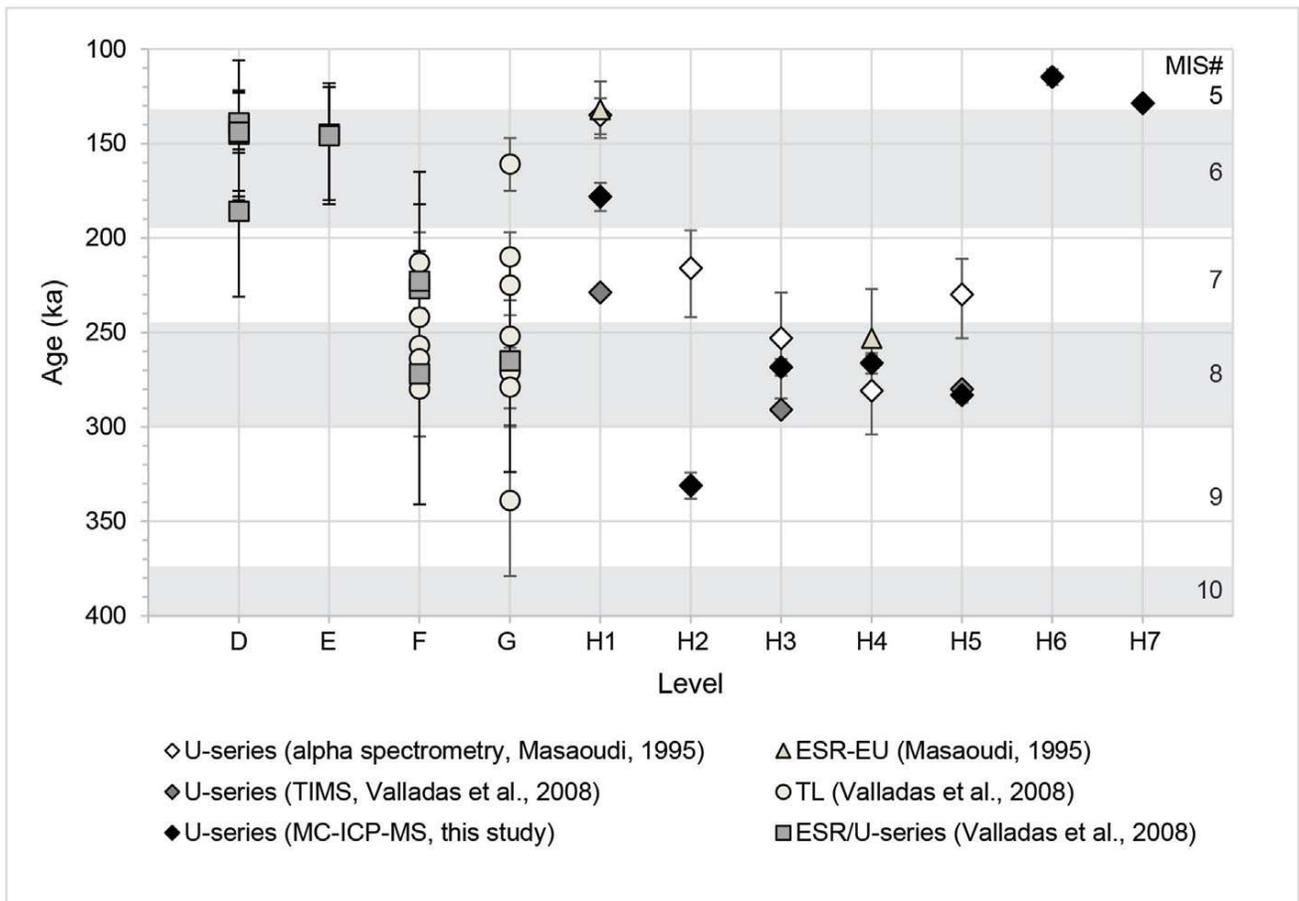
Fig. 10. Payre. Synthesis of the new and previous ages obtained. For some of the U-series ages, error bars are not visible due to the scale.

4. Discussion

The new ages obtained for the Middle Palaeolithic sites of the Middle Rhône valley are presented in Fig. 9. They range from ca. 500 ka (maximum age obtained from the soda straws from Abri du Maras) to ca. 13 ka (minimum age obtained from bone at Grotte du Figuier). Due to issues related to the presence of exogeneous thorium that contaminated the samples, most of the apparent ages obtained using U-series on bones should be used with caution.

Fig. 10 presents a synthesis of ages obtained in Payre (see Tables 1 and 3). None of the U-series ages obtained from the flowstone follows the stratigraphic order, likely due to diagenesis. They span MIS 10 to 5, but the inverse relation between apparent ages and U-content observed in our samples (Fig. 5a) suggests U mobility and an open system (see discussion in Pons-Branchu et al., 2020). The top of the flowstone (H1), overlying level G, yielded an age of 178 ± 8 ka (sample #18). This age is younger than the age obtained using TIMS by Valladas et al. (2008), of 229 ± 2 ka and older than the one obtained by alpha spectrometry and ESR by Masaoudi (1995) (see details in Table 1). For H2, our U-series age is also older than ESR age, suggesting a complex diagenetic history for the upper part of the flowstone. For H5, the TIMS U-series ages of 280 ± 3 ka obtained falls within the same range than our new age, of 283 ± 4 ka. The average TL ages published by Valladas et al. (2008) for levels G (247 ± 29 ka) and F (251 ± 25 ka) suggest that the human occupation of these levels occurred during the same time interval (end of MIS 8-beginning of MIS 7), in agreement with ESR/U-series on teeth and bones, ranging from 139 ± 16 ka (D) and 265 ± 59 ka (G). As shown in Fig. 10, some of the ages obtained from the flowstone are younger than the TL ages for overlying layer G (H1, H6 and H7) or fall within the same range (H2, H3, H4, H5). An overestimation of TL ages due to partial bleaching of the TL signal is unlikely considering that the flint samples were selected after ensuring that their signal was reset, due to exposition to a temperature >450 °C. However, for level G, one age appears older (339 ± 40 ka). Valladas et al. (2008) raised the possibility of an incorrect assessment of the external dose rate, which may vary in layer G, partially brecciated. Considering the issues mentioned above and taking into account all available ages for Payre, the occupation of the cave likely occurred between MIS 9 and 6 (Fig. 10). At Ranc-Pointu 2, the corrected ^{230}Th/U age obtained from the overlying flowstone (RCP2), of 110 ± 9 ka, is in agreement with the IRSL age obtained for the archaeological layer c (WLL921), of 145 ± 9 ka (Table 1), and follows the stratigraphic order. It suggests an occupation time at the end of the Middle Pleistocene, during MIS 6, which would be contemporary with human activity at the top of the sequence at Payre. The two other ages were obtained from residual flowstones that can hardly be contextualised in the sequence. However, they suggest that good conditions occurred for flowstone formation during the second half of MIS 5 (RCP3, 85 ± 3 ka) and the beginning of MIS 3 (RCP1, 57 ± 0.5 ka).

The U-series ages obtained from the tooth at Baume Flandin suggest that human occupation took place at least 106 ka (minimum estimate: 108.8 ± 2.1 ka), during the first half of MIS 5. MIS 5e occupations are rare in the region and can be correlated with level u at Saint-Marcel cave with *Dama dama* remains (Moncel et al., 2010, 2015).

The two ESR/U-series ages obtained for the Abri du Maras (layer 4.2), of 42 ± 3 ka and 42 ± 6 ka, are similar to those previously obtained for layers 4.1 and 4.2, ranging from 55 ± 2 ka to 40 ± 3 (Table 1 and SOM Table S2). Together with the IRSL age of 46 ± 4 ka, they confirm the attribution of this part of the archaeological sequence to MIS 3 and frame these occupations among the latest associated with Neanderthals in the area (Szmidt et al., 2010; Richard et al., 2015). The U-series dates obtained from the soda straws (>200 ka) from layers upper 5 and 6 must be considered as a terminus post quem. Except for the IRSL age of 63 ± 3 ka (layer 4.1) and of 51 ± 3 ka (layer 6), which do not follow the stratigraphic order probably due to dosimetric hereogeneity, the absence of in-situ measurements and/or bleaching issues, the new age results obtained on layer 4 (4.1 and 4.2), coeval with MIS 3, are in general agreement with those previously published by Moncel and Michel (2000) on layer 5, ranging from 91 ± 4 ka to 72 ± 3 ka. Moreover, the age of 90 ± 9 ka obtained using ESR/U-series on layer upper 5 (Richard et al., 2015) supports the attribution of the base of the sequence to MIS 5.

The numerous dates obtained at the Abri des Pêcheurs since the 1980s suggest an occupation after MIS 5, from the end of MIS 4 to MIS 3. The new U-series ages obtained from bones, of 23 ± 9 ka and 22 ± 4 ka, only provide minimum estimates (as previous U-series ages obtained from bones using alpha spectrometry, Masaoudi et al., 1994, Table 1), and are problematic considering the issue of exogeneous Th contamination (^{230}Th/^{232}Th < 4). The flowstone previously dated (see Table 1) provides a maximum age estimate for the overlying sequence. The base of the flowstone was dated to 400 ± 24 ka (Richard et al., 2015) and U-series ages obtained from the youngest part of the flowstone range from 110 ± 15 ka (Richard et al., 2015) to 83 ± 6 ka (Masaoudi et al., 1994). Considering the maximum age obtained from the upper part of the flowstone, human occupation likely occurred after MIS 5. Moreover, a tooth was dated to 54 ± 5 ka using ESR/U-series (Richard et al., 2015) and radiocarbon ages are ca. 30000-25000 years BP (Evin et al., 1985). At Grotte du Figuier, sedimentological studies suggest that layer 4 in rooms 1 and 2 are correlated (Moncel et al., 2012b). Nonetheless, the ESR/U-series age obtained in room 1, layer 4, of 52 ± 9 ka (Richard et al., 2015), is older than the age of 29 ± 4 ka (FIG-373) but falls within the same range as 40 ± 4 ka (FIG-405). Moreover, U-series corrected ages obtained from one bone and one tooth, of 34 ± 7 ka (FIG 24) and 13 ± 1 ka (FIG 36), only provide a minimum estimate. The contemporaneity of layer 4 in the two rooms is thus not confirmed in light of these data. The ESR (Ti-Li) ages obtained on the sediment sampled in layer 1 (micaceous sand at the base of the sequence), of 378 ± 30 and 305 ± 36 ka (MIS 11-8), may give a maximum age estimate for the
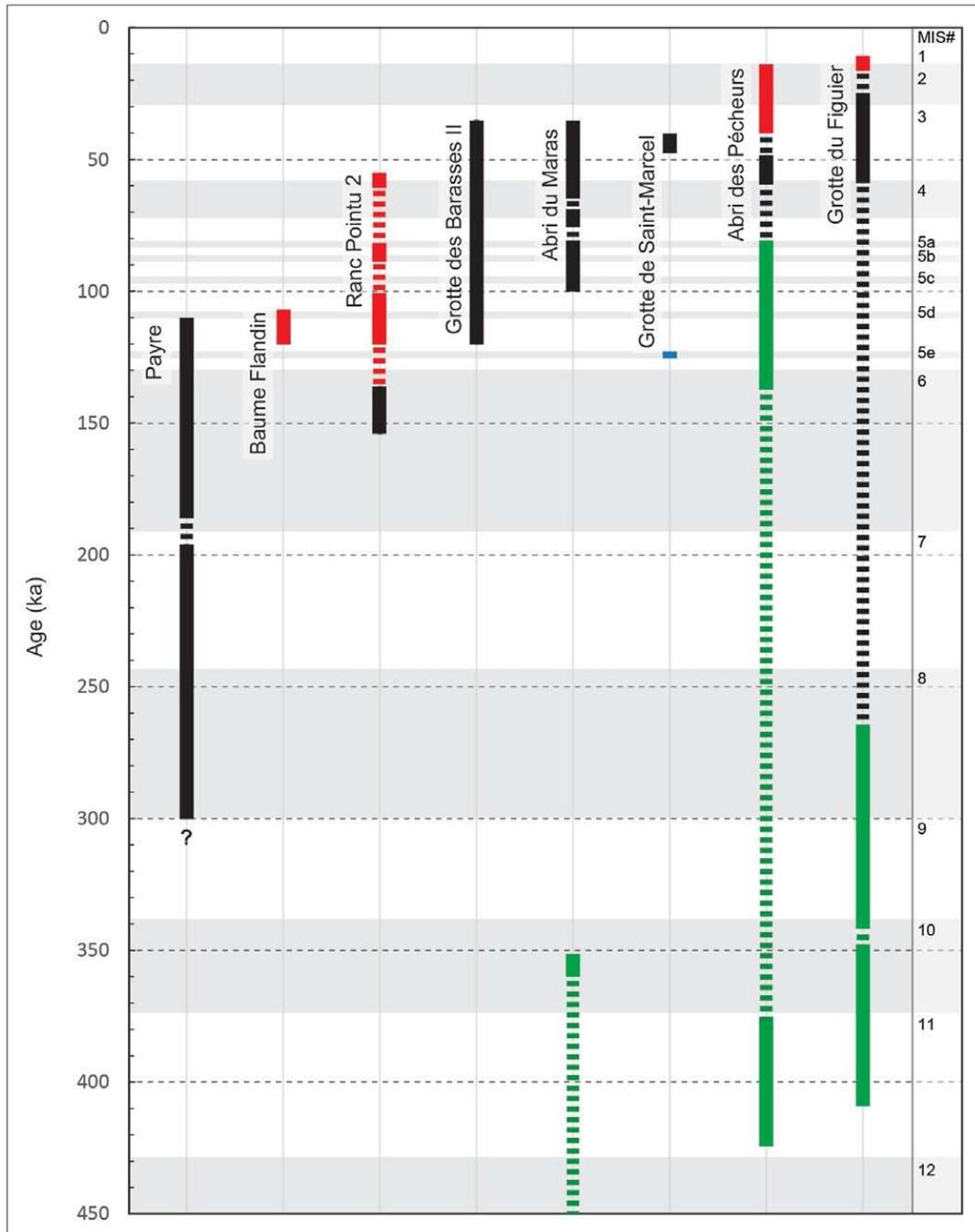
overlying layers.

Fig. 11. Duration of occupation based on the previous data presented in Table 1 and the new ages obtained in this study. The minimum/maximum age estimates for the human occupation are presented in red and green, respectively. The biochronology appears in blue. Hiatuses are represented by dashed lines.

5. Cultural interpretations

Fig. 11 represents the duration of occupation in the studied sites, together with other major caves in the region, Grotte des Barasses II and Grotte de Saint-Marcel. Most of the archaeological layers are dated to the Late Pleistocene (end of MIS 5, MIS 4 and 3) and there is little evidence of MIS 7, MIS 6 and MIS 5e occupations. In the current state of knowledge, occupations in the area begins at Orgnac 3 (MIS 9-8) and the latest evidences of Middle Palaeolithic-type assemblages are dated so far to MIS 3, between 37 and 40 ka, at the Ranc de l'Arc, Saint-Marcel, Abri des Pêcheurs and Abri du Maras (Defleur et al., 1990; Szmidt et al., 2010; Richard et al., 2015). The density of occupation seems to be higher during the Late Middle Palaeolithic according to the current data. Sedimentation in cave and shelter settings records spots and palimpsests of occupations, and discontinuity in deposits that can be related only to general MIS phases, as opposed to open-air occupation in alluvial contexts (north-west of France). However, the diversity of proxies (pollens, macrofauna, microfauna and molluscs), when applicable to these sites, allows describing the environmental context of the human occupation as a mosaic of vegetation around sites (forested patches and meadows). Moreover, most of the results of these proxies are in agreement with the proposed chronology. Neanderthal presence seems to be uninterrupted in this southern area, regardless of climatic conditions, adapted to the diversity of species (one or several ones during short or long-term occupations) living around the habitat, and moved possibly according to the available biomass. Long sequences covering several MIS are rare (Payre for instance) suggesting taphonomic processes with erosion phases at the sites and/or evolution of caves and shelters over time that did not permit occupations over long periods (collapse of the roof and the entrance).

Neanderthals occupied various types of habitat, from narrow caves to vast shelters, along the rivers or in the low plateaus along the Rhodanian corridor. Any topographic barrier could have stopped human mobility between valleys and plateaus and access to higher altitudes (Massif Central mountains). To date, most of the remains are located in limestone formations allowing preservation of occupations into caves and few open-air sites have been found (Bernard-Guelle et al., 2011; Burke et al., 2021). A large part of Neanderthal activities and occupations are therefore unknown and it is unclear whether the climatic context could have affected the intensity of occupations, the land use patterns and choices of type of habitat.

If we summarize the technological and typological behaviours in the updated chronological framework, the archaeological record attests the earliest evidence of laminar volumetric technology on slabs during MIS 5e (Baume Flandin), common in the South of France while it is observed earlier, starting from MIS 8, in the North-West part (Tuffreau, 1993). This technology is associated at the Baume Flandin with a Levallois core technology including various methods (unipolar and centripetal) for producing flakes, points and elongated

flakes/blades. The use of a Levallois core technology starts earlier in the area in the sequence of the site of Orgnac 3 (MIS 9e8) with a main centripetal method, and it remains common in some sequences from MIS 5 to 3, mainly with a unipolar method (Baume Flandin and Abri du Maras for instance). It is also observed at the Abri Moula and Baume Néron during MIS 4 and 3 (Defleur et al., 1994; Defleur, 2015). At Payre it is very punctual, perhaps in the form of some introduced flakes. The discoid-type core technology is common from Payre (MIS 7-6) to MIS 3 sites (Saint-Marcel, Abri des Pêcheurs, Barasses II, Grotte du Figuier), associated in some instances to the Levallois and other types of technology. The chronology of a site cannot be based on technological organisation because similar strategies exist over time in various contexts. The main core technology and the secondary technologies for each occupation attest the diversity of "know-how" of Neanderthal populations from MIS 7 to 3, and possibly the selection of some methods depending on the activities and needs. There is no relationship with the regional subsistence behaviours (foraging/circulating model) or the duration of the occupations (Binford, 1981). The duration of occupation explains rather the composition of the assemblage, opposing bivouacs with a mainly introduced lithic component associated to a limited debitage in situ, to longer occupations with both introduction and production of material in situ. The subsistence strategies are more related to cave size, opposing narrow and small caves occupied as bivouacs to large caves and shelters used for long and short-term seasonal occupations.

For the tool kits, most of the assemblages are composed of scrapers and points mainly made on flakes or elongated points, with a limited retouch and little evidence of resharpening. Blades are in general slightly retouched, as are Levallois products. The Quina Rhodanian facies remains rare with original features compared to the eponym source located in the South-West part of France. The retouch is more "semi-Quina" than "Quina" on scrapers and convergent scrapers, and concerns flakes and elongated flakes produced by various methods.

Flint is the main raw material, in an area rich in chert outcrops, especially in the limestone plateaus. The detailed studies show a perimeter of territory of gathering varying between 30 and 60 km with a collection of local and semi-local flint under various forms. Neanderthals had a behaviour of "collector", gathering all types of flint in alluvial and colluvial formations in the valleys or on the plateaus (Fernandes et al., 2008). Some long-distance flints were introduced already worked (Payre and Abri du Maras for seasonal occupations with a main local and semi-local gathering) and the function of the site (bivouacs for Abri des Pêcheurs and Barasses II with a lot of flint types and a large perimeter of gathering) partially explains the diversity of land-use patterns over time in the region.

Finally, we can mention the punctual use of other raw materials for a complementary debitage (on quartz and limestone by Levallois or other methods) without clear functional reasons or during the early Middle

Palaeolithic for some large cutting tools and pebble-tools (basalt, limestone, quartzite). Pieces made from these rocks are introduced already worked or were made *in situ*.

6. Conclusion

The new investigations in the Middle Rhône Valley in the last twenty years allowed the revision of archaeological, geological and chronological data for the study of Neanderthal settlement patterns during the Middle and Late Pleistocene. The 43 new age determinations presented herein, together with 77 previous ages, allow framing Neanderthal behaviour, from the early phase of the Middle Palaeolithic, documented in Payre ca. 300 ka (MIS 8), to the latest phases during the second half of MIS 3, ca. 40 ka, at Abri du Maras, Grotte des Barasses II, Abri des Pêcheurs, Grotte de Saint-Marcel and Grotte du Figuier. Occupations during MIS 7, 6 and 5 seem to be also recorded in Payre, Baume Flandin and Ranc-Pointu 2. These results suggest a continuous exploitation of the area by Neanderthal groups from the late Middle Pleistocene (e.g., in Orgnac and Payre) to the arrival of modern humans around 36000 years cal BP (in Chauvet Cave, Valladas et al., 2001; Quiles et al., 2013; Quiles et al., 2016).

The reappraisal of archaeological data, together with an updated chronology, allows shedding more light into the diversity of human occupations in the southeastern margins of the Massif Central. The region may have been an important pathway connecting northern to southern Europe during the Middle Palaeolithic, documenting one of the oldest examples of Levallois technology at ca. 300 ka in Orgnac, and during the Upper Palaeolithic too, considering that this area is one of the earliest occupied by modern humans in southern Europe.

Supplementary data to this article can be found online at
https://doi.org/10.1016/j.quascirev.2021.107241.

References

Adamiec, G., Aitken, M.J., 1998. Dose-rate conversion factors: update. Ancient TL 16, 37-50.

Argant, J., Brochier, J.-L., Mandier, P., Petiot, P., 1991. In: Le cône détritique de la Drôme : une contribution à la connaissance de l'Holocène du Sud-Est de la France. Quaternaire, pp. 83-99.

Baena, J., Moncel, M.-H., Cuartero, F., Chacón Navarro, M.G., Rubio, D., 2017. Late middle Pleistocene genesis of neanderthal technology in western Europe: the case of Payre site (south-east France). Quat. Int. 436, 212-238.

Bernard-Guelle, S., 2005. Territoires et mobilité des groupes moustériens en Vercors : analyse et discussion. L'Anthropologie 109, 799-814.

Bernard-Guelle, S., Rué, M., Fernandes, P., Courty, M.-A., Piboule, M., Coudenneau, A., Argant, J., Picavet, R., Dawson, M.-C., 2011. Le site moustérien d'Andance (Saint-Bauzile, Ardèche): un habitat de hauteur en contexte basaltique dans la moyenne vallée du Rhône. Bull. Soc. Prehist. Fr. 108, 671-695.

Binford, L.R., 1981. In: Bones: Ancient Men and Modern Myths. Academic press, New York, p. 320.

Bocherens, H., Díaz-Zorita Bonilla, M., Daujeard, C., Fernandes, P., Raynal, J.-P., Moncel, M.-H., 2016. Direct isotopic evidence for subsistence variability in Middle Pleistocene Neanderthals (Payre, southeastern France). Quat. Sci. Rev. 154, 226-236.

Bourguignon, L., 1997. Le Moustérien de type Quina: nouvelle définition d'une
technique. PhD thesis. Université de Paris X, Nanterre.

Bouvier, P., 1982. Deux canines néandertaliennes: Jaurens à Nespouls (Corrèze) et Casteljau (Ardèche). Nouv. Arch. Mus. Hist. Nat. Lyon 20 (Supplément), 17-21.

Brennan, B.J., 2003. Beta doses to spherical grains. Radiat. Meas. 37, 299-303.

Brennan, B.J., Lyons, R.G., Phillips, S.W., 1991. Attenuation of alpha particle track dose for spherical grains. Int. J. Radiat. Appl. Instrum. Nucl. Tracks Radiat. Meas. 18, 249-253.

Brennan, B.J., Rink, W.J., McGuirl, E.L., Schwarcz, H.P., Prestwich, W.V., 1997. Beta doses in tooth enamel by "one-group" theory and the ROSY ESR dating software. Radiat. Meas. 27, 307-314.

Burdette, K.E., Rink, W.J., Mallinson, D.J., Means, G.H., Parham, P.R., 2013. Electron spin resonance optical dating of marine, estuarine, and aeolian sediments in Florida, USA. Quat. Res. 79, 66-74.

Burke, A., Moncel, M.-H., Cattin, M.-I., Chomette, D., Paquin, S., 2021. Prospections archéologiques dans la région de la vallée de l'Eyrieux, Ardèche. Ardèche Archéologie 38, 3-13.

Carmignani, L., Moncel, M.-H., Fernandes, P., Wilson, L., 2017. Technological variability during the Early Middle Palaeolithic in Western Europe. Reduction systems and predetermined products at the Bau de

l'Aubesier and Payre (South- East France). PLoS One 12, e0178550.

Chacón, M.G., Détroit, F., Coudenneau, A., Moncel, M.-H., 2016. Morphometric assessment of convergent tool technology and function during the early middle palaeolithic: the case of Payre, France. PLoS One 11, e0155316.

Cheng, H., Lawrence Edwards, R., Shen, C.-C., Polyak, V.J., Asmerom, Y., Woodhead, J., Hellstrom, J., Wang, Y., Kong, X., Spötl, C., Wang, X., Calvin Alexander, E., 2013. Improvements in ^{230}Th dating, ^{230}Th and ^{234}U half-life values, and U-Th isotopic measurements by multi-collector inductively coupled plasma mass spectrometry. Earth Planet Sci. Lett. 371e372, 82-91.

Combier, J., 1967. Le Paléolithique de l'Ardèche dans son cadre paléoclimatique, Publication de l'Institut de Préhistoire de l'Université de Bordeaux vol. 4. Delmas, p. 463.

Combier, J., 1968. Rapport sur la campagne de fouilles à Balazuc, Ardèche. Circonscription archéologique Rhône-Alpes (inédit).

Crégut-Bonnoure, E., Boulbes, N., Daujeard, C., Fernandez, P., Valensi, P., 2010. Nouvelles données sur la grande faune de l'Eémien dans le Sud-Est de la France. Quaternaire. Revue de l'Association française pour l'étude du Quaternaire 21, 227-248.

Daffara, S., Borel, A., Moncel, M.-H., 2019. Conditioning of the raw materials on discoid exploitation strategies during the Early Middle Palaeolithic: the example of Payre level D (South-East France). Archaeological and Anthropological Sciences 11, 4681-4695.

Daujeard, C., 2018. In: La Grotte des Barasses II (Balazuc, Ardèche): entre

néandertaliens, bouquetins et carnivores. Des occupations du Pléistocène supérieur en moyenne vallée de l'Ardèche. Editions DARA, Lyon, p. 210.

Daujeard, C., Moncel, M.-H., 2010. On Neanderthal subsistence strategies and land use: a regional focus on the Rhone Valley area in southeastern France.

J. Anthropol. Archaeol. 29, 368-391.

Daujeard, C., Moncel, M.-H., Rivals, F., Fernandez, P., Auguste, P., Aureli, D., Bocherens, H., Crégut-Bonnoure, E., Debard, E., Liouville, M., 2011. Quel type d'occupation dans l'ensemble F de Payre (Ardèche, France) ? Halte de chasse spécialisée ou campement de courte durée ? Un exemple d'approche multidisciplinaire. In: Costamagno, S., Bon, F., Valdeyron, N. (Eds.), Les Haltes de chasse en préhistoire : Quelles réalités archéologiques ? P@lethnologie, Toulouse (13-15 mai 2009), pp. 77-103.

Daujeard, C., Fernandes, P., Guadelli, J.-L., Moncel, M.-H., Santagata, C., Raynal, J.-P., 2012. Neanderthal subsistence strategies in southeastern France between the plains of the Rhone valley and the mid-mountains of the Massif central (MIS 7 to MIS 3). Quat. Int. 252, 32-47.

Daujeard, C., Daschek, E.J., Patou-Mathis, M., Moncel, M.H., 2018. Les néandertaliens de Payre (Ardèche, France) ont-ils chassé le rhinocéros? Quaternaire. Revue de l'Association française pour l'étude du Quaternaire 29, 217-231.

Daujeard, C., Brugal, J.-P., Moncel, M.-H., Fernandes, P., Delvigne, V., Lafarge, A., Le Pape, J.-M., Raynal, J.-P., 2019a. Neanderthals and caprines in two upper Pleistocene caves of southeastern France. In: Gourichon, L., Daujeard, C., Brugal, J.-P. (Eds.), Hommes et Caprinés. De la montagne à la steppe, de la chasse à l'élevage. XXXIXe rencontres internationales d'archéologie et d'histoire d'Antibes.
Éditions APDCA, Antibes, pp. 115-137.

Daujeard, C., Vettese, D., Britton, K., Béarez, P., Boulbes, N., Crégut-Bonnoure, E., Desclaux, E., Lateur, N., Pike-Tay, A., Rivals, F., Allué, E., Chacón, M.G., Puaud, S., Richard, M., Courty, M.A., Gallotti, R., Hardy, B., Bahain, J.J., Falguères, C., Pons- Branchu, E., Valladas, H., Moncel, M.H., 2019b. Neanderthal selective hunting of reindeer? The case study of Abri du Maras (south-eastern France). Archaeological and Anthropological Sciences 11, 985-1011.

Debard, E., 1988. In: Le Quaternaire du Bas-Vivarais: dynamique sédimentaire, paléoclimatologie et chronologie d'après l'étude sédimentologique des remplissages d'avens, de porches de grottes et d'abris sous roche: comparaisons avec le Velay oriental. PhD thesis, vol. 1. Université Claude Bernard, Lyon, p. 317. Defleur, A., Valladas, H., Radulescu, C., Combier, J., Arnold, M., 1990. Stratigraphie et datation carbone 14, en spectrométrie de masse par accélérateur, du Moustérien récent de l'abri du Ranc de l'Arc (Ardèche, France). Comptes Rendus de l'Académie des Sciences de Paris 311, 719-724.

Defleur, A., Bez, J.F., Crégut-Bonnoure, E., Fontugne, M., Jeannet, M., 1994. Industries, biostratigraphie, restes humains et datation du gisement moustérien de la Baume Néron (Soyons, Ardèche). Comptes rendus de l'Académie des sciences. Série 2. Sciences de la terre et des planètes 318, 1409-1414.

Defleur, A., 2015. Les industries lithiques moustériennes de la Baume Moula-Guercy (Soyons, ardèche). Fouilles 1993e1999. l'Anthropologie 119 (2), 170-253.

Duval, M., 2012. Dose response curve of the ESR signal of the Aluminum center in quartz grains extracted from sediment. Ancient TL 30, 41-50.

Duval, M., Guilarte, V., 2015. ESR dosimetry of optically bleached quartz grains extracted from Plio-Quaternary sediment: evaluating some key aspects of the ESR signals associated to the Ti-centers. Radiat. Meas. 78, 28-41.

Duval, M., Sancho, C., Calle, M., Guilarte, V., Pen~a-Monné, J.L., 2015. On the interest of using the multiple center approach in ESR dating of optically bleached quartz grains: some examples from the Early

Pleistocene terraces of the Alcanadre River (Ebro basin, Spain). Quat. Geochronol. 29, 58-69.

Ecker, M., Bocherens, H., Julien, M.-A., Rivals, F., Raynal, J.-P., Moncel, M.-H., 2013. Middle Pleistocene ecology and Neanderthal subsistence: insights from stable isotope analyses in Payre (Ardèche, southeastern France). J. Hum. Evol. 65, 363-373.

Edwards, L.R., Chen, J.H., Wasserburg, G.J., 1987. ^{238}U-^{234}U-^{230}Th-^{232}Th systematics and the precise measurement of time over the past 500,000 years. Earth Planet Sci. Lett. 81, 175-192.

El Hazzazi, N., 1998. In: Paléoenvironnement et chronologie des sites du Pleistocène

moyen et supérieur, Orgnac 3, Payre et Abri des Pêcheurs (Ardèche, France) d'après l'étude des rongeurs. PhD thesis. Muséum National d'Histoire Naturelle, p. 246.

Evin, J., Marechal, J., Marien, G., 1985. Lyon natural radiocarbon measurements X. Radiocarbon 27, 386e454.

Fernandes, P., Moncel, M.-H., Lhomme, G., 2010. Analyse des comportements face aux ressources minérales de deux sites du Paléolithique moyen : Payre, Abri des Pêcheurs (Ardèche, France). Rivista di Scienze Preistoriche LVII LVII, 31-42.

Fernandes, P., Raynal, J.-P., Moncel, M.-H., 2008. Middle Palaeolithic raw material gathering territories and human mobility in the southern Massif Central, France: first results from a petro-archaeological study on flint. J. Archaeol. Sci. 35, 2357-2370.

Foury, Y., Desclaux, E., Daujeard, C., Defleur, A., Moncel, M.-H., Raynal, J.-P., 2016. Evolution des faunes de rongeurs en moyenne vallée du Rhône (rive droite, Ardèche, France) au cours du pléistocène moyen final et du pléistocène supérieur ancien, du mis 6 au mis 4. Quaternaire. Revue de l'Association française pour l'étude du Quaternaire 27, 55-79.

Genty, D., Ghaleb, B., Plagnes, V., Causse, C., Valladas, H., Blamart, D., Massault, M., Geneste, J.-M., Clottes, J., 2004. Datations U/Th (TIMS) et 14C (AMS) des stalagmites de la grotte Chauvet (Ardèche, France) : intérêt pour la chronologie des événements naturels et anthropiques de la grotte. Comptes Rendus Palevol 3, 629-642.

Genuite, K., Delannoy, J.-J., Bahain, J.-J., Gresse, M., Jaillet, S., Phillippe, A., Pons-Branchu, E., Revil, A., Voinchet, P., 2021. Dating the landscape evolution around the Chauvet-Pont d'Arc cave. Sci. Rep. 11, 8944.

Grün, R., 1994. A cautionary note: use of 'water content'and 'depth for cosmic ray dose rate' in AGE and DATA programs. Ancient TL 12, 50-51.

Grün, R., 2000. Methods of dose determination using ESR spectra of tooth enamel. Radiat. Meas. 32, 767-772.

Grün, R., 2009. The DATA program for the calculation of ESR age estimates on tooth enamel. Quat. Geochronol. 4, 231-232.

Grün, R., Aubert, M., Joannes-Boyau, R., Moncel, M.-H., 2008. High resolution analysis of uranium and

thorium concentration as well as U-series isotope distributions in a Neanderthal tooth from Payre (Ardèche, France) using laser ablation ICP-MS. Geochem. Cosmochim. Acta 72, 5278-5290.

Grün, R., Eggins, S., Kinsley, L., Moseley, H., Sambridge, M., 2014. Laser ablation U- series analysis of fossil bones and teeth. Palaeogeogr. Palaeoclimatol. Palaeoecol. 416, 150-167.

Grün, R., Katzenberger-Apel, O., 1994. An alpha irradiator for ESR dating. Ancient TL 12, 35-38.

Grün, R., Schwarcz, H.P., Chadam, J., 1988. ESR dating of tooth enamel: coupled correction for U-uptake and U-series disequilibrium. Int. J. Radiat. Appl. Instrum. Nucl. Tracks Radiat. Meas. 14, 237-241.

Guillaud, E., Béarez, P., Daujeard, C., Defleur, A.R., Desclaux, E., Roselló-Izquierdo, E., Morales-Muñiz, A., Moncel, M.-H., 2021. Neanderthal foraging in freshwater ecosystems: a reappraisal of the Middle Paleolithic archaeological fish record from continental Western Europe. Quat. Sci. Rev. 252, 106731.

Hardy, B.L., Moncel, M.-H., 2011. Neanderthal use of fish, mammals, birds, starchy plants and wood 125-250,000 Years ago. PLoS One 6, e23768.

Hardy, B.L., Moncel, M.-H., Daujeard, C., Fernandes, P., Béarez, P., Desclaux, E.,

Chacon Navarro, M.G., Puaud, S., Gallotti, R., 2013. Impossible Neanderthals? Making string, throwing projectiles and catching small game during marine isotope stage 4 (abri du Maras, France). Quat. Sci. Rev. 82, 23-40.

Hardy, B.L., Moncel, M.H., Kerfant, C., Lebon, M., Bellot-Gurlet, L., Mélard, N., 2020.

Direct evidence of Neanderthal fibre technology and its cognitive and behavioral implications. Sci. Rep. 10, 4889.

Harmand, D., Adamson, K., Rixhon, G., Jaillet, S., Losson, B., Devos, A., Hez, G., Calvet, M., Audra, P., 2017. Relationships between fluvial evolution and karstification related to climatic, tectonic and eustatic forcing in temperate regions. Quat. Sci. Rev. 166, 38-56.

Hellstrom, J., 2003. Rapid and accurate U/Th dating using parallel ion-counting multi-collector ICP-MS. J. Anal. At. Spectrom. 18, 1346-1351.

Higham, T., Douka, K., Wood, R., Ramsey, C.B., Brock, F., Basell, L., Camps, M., Arrizabalaga, A., Baena, J., Barroso-Ruiz, C., Bergman, C., Boitard, C., Boscato, P., Caparros, M., Conard, N.J., Draily, C., Froment, A., Galvan, B., Gambassini, P., Garcia-Moreno, A., Grimaldi, S., Haesaerts, P., Holt, B., Iriarte-Chiapusso, M.-J., Jelinek, A., Jorda Pardo, J.F., Maillo-Fernandez, J.-M., Marom, A., Maroto, J., Menendez, M., Metz, L., Morin, E., Moroni, A., Negrino, F., Panagopoulou, E., Peresani, M., Pirson, S., de la Rasilla, M., Riel-Salvatore, J., Ronchitelli, A., Santamaria, D., Semal, P., Slimak, L., Soler, J., Soler, N., Villaluenga, A., Pinhasi, R., Jacobi, R., 2014. The timing and spatiotemporal patterning of Neanderthal disappearance. Nature 512, 306-309.

Huntley, D.J., Godfrey-Smith, D.I., Haskell, E.H., 1991. Light-induced emission spectra from some quartz and

feldspars. Int. J. Radiat. Appl. Instrum. Nucl. Tracks Radiat. Meas. 18, 127-131.

Huntley, D.J., Lamothe, M., 2011. Ubiquity of anomalous fading in K-feldspars and correction for it in optical dating. Can. J. Earth Sci. 38, 1093-1106.

Ivanovich, M., Harmon, R.S., 1992. In: Uranium-Series Disequilibrium: Applications to Earth, Marine, and Environmental Sciences (2nd edition). Clarendon Press, Oxford, p. 910.

Jaffey, A.H., Flynn, K.F., Glendenin, L.E., Bentley, W.C., Essling, A.M., 1971. Precision measurement of half-lives and specific activities of ^{40}U and ^{238}U. Phys. Rev. C 4, 1889-1906.

Kalaï, C., 1998. In: Reconstitution du paléoenvironnement végétal et du paléoclimat de la fin du Pléistocène moyen et du Pléistocène supérieur d'après les analyses polliniques de la Baume Moula-Guercy, du site de Payre et de l'abri des Pêcheurs (Ardèche, France). PhD thesis. Muséum National d'Histoire Naturelle, p. 175.

Kalaï, C., Moncel, C., Miskovsky, J., 2001. Le paléoenvironnement végétal des occupations humaines de la grotte de Payre à la fin du Pleistocène moyen et au début du Pléistocène supérieur (Ardèche, France). Trab. Prehist. 58, 143-151.

Laurent, M., Falguères, C., Bahain, J.J., Rousseau, L., Van Vliet Lanoé, B., 1998. ESR dating of quartz extracted from quaternary and neogene sediments: method, potential and actual limits. Quat. Sci. Rev. 17, 1057-1062.

Lees, S., 1987. Considerations regarding the structure of the mammalian mineralized osteoid from viewpoint of the generalized packing model. Connect. Tissue Res. 16, 281-303.

Ludwig, K., 2003. In: User's Manual for ISOPLOT/Ex 3.00. A Geochronological Toolkit for Microsoft Excel. Berkeley Geochronology Center Special Publication, 4, Berkeley, pp. 1-70.

Mandier, P., 1984. Signification dynamique et climatique des formations et terrasses fluviatiles quaternaires dans les Alpes et leur périphérie. Quaternaire 113-118.

Marín, J., Daujeard, C., Saladié, P., Rodríguez-Hidalgo, A., Vettese, D., Rivals, F., Boulbes, N., Crégut-Bonnoure, E., Lateur, N., Gallotti, R., Arbez, L., Puaud, S., Moncel, M.-H., 2020. Neanderthal faunal exploitation and settlement dynamics at the Abri du Maras, level 5 (south-eastern France). Quat. Sci. Rev. 243, 106472.

Masaoudi, H., 1995. In: Application des méthodes du déséquilibre des familles de l'uranium (^{230}Th/^{234}U) et de la résonance de spin éléctronique (ESR) à la datation des sites d'Orgnac 3, de Payre et de l'abri des Pêcheurs (Ardèche). PhD thesis. Muséum national d'histoire naturelle, Paris, p. 155.

Masaoudi, H., Falguères, C., Bahain, J.-J., Yokohama, Y., Lhomme, G., 1994. Datation d'ossements et de planchers stalagmitiques provenant de l'Abri des Pêcheurs (Ardèche) par la méthode des déséquilibres des familles de l'uranium (U-Th). Quaternaire 5, 79-83.

Mercier, N., Falguères, C., 2007. Field gamma dose-rate measurement with a NaI(Tl) detector: re-evaluation of the "threshold" technique. Ancient TL 25, 1-4.

Michel, V., Shen, G., Shen, C.-C., Wu, C.-C., Vérati, C., Gallet, S., Moncel, M.-H., Combier, J., Khatib, S., Manetti, M., 2013. Application of U/Th and $^{40}Ar/^{39}Ar$ dating to orgnac 3, a late acheulean and early middle palaeolithic site in ardèche, France. PLoS One 8, e82394.

Millard, A.R., Hedges, R.E.M., 1995. The role of the environment in uranium uptake by buried bone. J. Archaeol. Sci. 22, 239-250.

Miras, Y., Barbier-Pain, D., Ejarque, A., Allain, E., Allué, E., Marín, J., Vettese, D., Hardy, B., Puaud, S., Mangado Llach, J., Moncel, M.-H., 2020. Neanderthal plant use and stone tool function investigated through non-pollen palynomorphs analyses and pollen washes in the Abri du Maras, South-East France. J. Archaeol. Sci.: Report 33, 102569.

Moncel, M.-H., 1994. In: L'industrie lithique des trois niveaux supérieurs de l'abri du Maras (Ardèche), Actes de la table ronde : les industries laminaires au Paléolitique moyen, dossier de documentation archéologique n° 18. CNRS éditions, Paris, pp. 118-123.

Moncel, M.-H., Gaillard, C., Patou-Mathis, M., 1994. L'abri du Maras (Ardèche) : une nouvelle campagne de fouilles dans un site paléolithique moyen (1993). BSPF, t 91 (n° 6), 363-369.

Moncel, M.-H., 1996. L'industrie lithique paléolithique moyen de l'abri du Maras (Ardèche). La question des Moustériens tardifs et du débitage laminaire au Paléolithique moyen. Gall. Prehist. 38, 1-41.

Moncel, M.-H., 2005. Baume Flandin et Abri du Maras : deux exemples de débitage laminaire du début du Pléistocène supérieur dans la Vallée du Rhône (sud-est, France). L'Anthropologie 109, 451e480.

Moncel, M.-H., 2008. In: Payre. Des occupations humaines de la moyenne vallée du Rhône de la fin du Pléistocène moyen et du début du Pléistocène supérieur. Mémoire de la Société Préhistorique Française, p. 336.

Moncel, M.H., Allué, E., Bailon, S., Barshay Szmidt, C., Béarez, P., Crégut, É.,

Daujeard, C., Desclaux, E., Debard, É., Lartigot Campin, A.S., Puaud, S., Roger, T., 2015. Evaluating the integrity of palaeoenvironmental and archaeological records in MIS 5 to 3 karst sequences from southeastern France. Quat. Int. 378, 22-39.

Moncel, M.-H., Borel, A., De Lombera, A., Sala, R., Deniaux, B., 2008a. Quartz et quartzite dans le site de Payre (MIS 7 et 5, Ardèche, France) : données techno- économiques sur la gestion de roches locales au Paléolithique moyen. Comptes Rendus Palevol 7, 441-451.

Moncel, M.-H., Brugal, J.-P., Prucca, A., Lhomme, G., 2008b. Mixed occupation during the middle palaeolithic: case study of a small pit-cave-site of les Pêcheurs (ardèche, south-eastern France). J. Anthropol. Archaeol. 27, 382-398.

Moncel, M.-H., Chacón, M.G., Coudenneau, A., Fernandes, P., 2009. Points and convergent tools in the European early Middle Palaeolithic site of Payre (SE, France). J. Archaeol. Sci. 36, 1892-1909.

Moncel, M.-H., Chacón, M.G., Vettese, D., Courty, M.-A., Daujeard, C., Eixea, A., Fernandes, P., Allué, E., Hardy, B., Rivals, F., Béarez, P., Gallotti, R., Puaud, S., 2021. Late Neanderthals short-term and specialized occupations at the Abri du Maras (South-East France, level 4.1, MIS 3). Anthropological and Archaeological Sciences 13, 45.

Moncel, M.-H., Condemi, S., 1996. Découverte de dents humaines dans le site Paléolithique moyen de Payre (Ardèche, France). Comptes rendus de l'Académie des sciences. Série 2. Sciences de la terre et des planètes 322, 251-257.

Moncel, M.-H., Condemi, S., 1997. Des restes humains dans le site paléolithique moyen ancien de Payre (Ardèche) : dents et pariétal -Nouvelles découvertes de 1996-. Bull. Soc. Prehist. Fr. 94, 168-171.

Moncel, M.H., Crégut Bonnoure, É., Daujeard, C., Lartigot, A.S., Lebon, M., Puaud, S., Boulbes, N., Croizet, S., 2008c. Le site de la baume Flandin (commune d'Orgnac- l'Aven) : nouvelles données sur ce gisement du Paléolithique moyen. Comptes Rendus Palevol 7, 315-325.

Moncel, M.-h., Daujeard, C., 2012. The variability of the Middle Palaeolithic on the right bank of the Middle Rhône Valley (southeast France): technical traditions or functional choices? Quat. Int. 247, 103e124.

Moncel, M.H., Daujeard, C., Cregut Bonnoure, É., Boulbes, N., Puaud, S., Debard, É., Bailon, S., Desclaux, E., Escude, É., Roger, T., Dubar, M., 2010. Nouvelles données sur les occupations humaines du début du Pléistocène supérieur de la moyenne vallée du Rhône (France). Les sites de l'Abri des Pêcheurs, de la Baume Flandin, de l'Abri du Maras et de la Grotte du Figuier (Ardèche). Quaternaire 21, 385-411.

Moncel, M.-H., Daujeard, C., Crégut-Bonnoure, E., Fernandez, P., Faure, M., Guérin, C., 2004. L'occupation de la grotte de Saint-Marcel (Ardèche, France) au Paléolithique moyen: stratégie d'exploitation de l'environnement et type d'occupation de la grotte. L'exemple des couches i, j et j'. Bull. Soc. Prehist. Fr. 257-304.

Moncel, M.-H., Débard, E., Desclaux, E., Dubois, J.-M., Lamarque, F., Patou- Mathis, M., Vilette, P., 2002. Le cadre de vie des hommes du Paléolithique moyen (stades isotopiques 6 et 5) dans le site de Payre (Rompon, Ardèche) : d'une grotte à un abri sous roche effondré. Bulletin de la Société préhistorique française Tome 99, 249-275.

Moncel, M.-H., Fernandes, P., Navarro, M.G.C., de Lombera Hermida, A., Menéndez Granda, L., Youcef, S., Moigne, A.-M., Patou-Mathis, M., Daujeard, C., Rivals, F., Valladas, H., Mercier, N., Bahain, J.-J., Voinchet, P., Falguères, C., Michel, V., Guanjun, S., Yokoyama, Y., Combier, J., 2014a. Emergence et diversification des stratégies au Paléolithique moyen ancien (350 000 à 120 000 ans)

dans la Vallée du Rhône (France). In: Jaubert, J., Froment, N., Depapepe, P. (Eds.), XXVIIème congrès CPF Transitions, ruptures et continuité en Préhistoire. Société Préhistorique Française, Bordeaux, pp. 43-59.

Moncel, M.-H., Lhomme, G., 2007. Les assemblages lithiques des niveaux du Paléolithique moyen de l'Abri des Pêcheurs (Ardèche, Sud-Est de la France): des occupations néandertaliennes récurrentes dans un « fossé ». L'Anthropologie 111, 211-253.

Moncel, M.-H., Michel, V., 2000. In: Première datation radiométrique par U-Th d'un niveau moustérien de l'Abri du Maras (Ardèche, France). Bulletin de la Société préhistorique française, pp. 371-375.

Moncel, M.-H., Moigne, A.-M., Combier, J., 2005. Pre-Neandertal behaviour during isotopic stage 9 and the beginning of stage 8. New data concerning fauna and lithics in the different occupation levels of Orgnac 3 (Ardèche, South-East France): occupation types. J. Archaeol. Sci. 32, 1283-1301.

Moncel, M.-H., Moigne, A.-M., Combier, J., 2012a. Towards the middle palaeolithic in western Europe: the case of orgnac 3 (southeastern France). J. Hum. Evol. 63, 653-666.

Moncel, M.-H., Moigne, A.-M., Sam, Y., Combier, J., Ashton, N., Díez, C., Monnier, G., Rolland, N., Sala Ramos, R., Szmidt, C.C., 2011. The emergence of Neanderthal technical behavior: new evidence from Orgnac 3 (Level 1, MIS 8), southeastern France. Curr. Anthropol. 52, 37-75.

Moncel, M.H., Puaud, S., Daujeard, C., Lartigot Campin, A.S., Millet, J.J., Theodoropoulou, A., Cregut Bonnoure, É., Gely, B., Vercoutère, C., Desclaux, E., Roger, T., Bourges, F., 2012b. La Grotte du Figuier (Saint-Martin-d'Ardèche) : bilan des travaux récents sur un site du Paléolithique moyen et supérieur de la moyenne vallée du Rhône (Sud-Est de la France). Bull. Soc. Prehist. Fr. 109, 35-67.

Moncel, M.H., Puaud, S., Daujeard, C., Lateur, N., Lartigot Campin, A.S., Debard, É., Crégut Bonnoure, É., Raynal, J.P., 2014b. Le site du Ranc-Pointu n° 2 à Saint-Martin-d'Ardèche : une occupation du Paléolithique moyen ancien dans le Sud- Est de la France. Comptes Rendus Palevol 13, 121-136.

Moncel, M., 2011. Technological behaviour and mobility of human groups through lithic assemblages at the end of Middle Pleistocene and beginning of Upper Pleistocene: the middle Rhône Valley case (France). In: Conard, N.J., Richter, J. (Eds.), Neanderthal Lifeways, Subsistence and Technology, 150 Years of Neanderthal Discoveries, vol. II. Spinger, New-York, pp. 261-289.

Moncel, M.H., Chacon, M.G., La Porta, A., Fernandes, P., Hardy, B., Gallotti, R., 2014c. Fragmented reduction processes: middle Palaeolithic technical behaviour in the Abri du Maras shelter, southeastern France. Quat. Int. 350, 180-204.

Murray, A.S., Roberts, R.G., 1997. Determining the burial time of single grains of quartz using optically stimulated luminescence. Earth Planet Sci. Lett. 152, 163-180.

Pedergnana, A., Ollé, A., Borel, A., Moncel, M.-H., 2018. Microwear study of quartzite artefacts: preliminary results from the Middle Pleistocene site of Payre (South-eastern France). Archaeological and Anthropological Sciences 10, 369-388.

Pons-Branchu, E., Douville, E., Roy-Barman, M., Dumont, E., Branchu, P., Thil, F., Frank, N., Bordier, L., Borst, W., 2014. A geochemical perspective on Parisian urban history based on UeTh dating, laminae counting and yttrium and REE concentrations of recent carbonates in underground aqueducts. Quat. Geochronol. 24, 44-53.

Pons-Branchu, E., Sanchidri´an, J.L., Fontugne, M., Medina-Alcaide, M.A., Quiles, A., Thil, F., Valladas Sanchidria´n, H., 2020. U-series dating at Nerja cave reveal open system. Questioning the Neanderthal origin of Spanish rock art. J. Archaeol. Sci. 117, 105120.

Prescott, J.R., Hutton, J.T., 1994. Cosmic ray contributions to dose rates for luminescence and ESR dating: large depths and long-term time variations. Radiat. Meas. 23, 497-500.

Price, Gilbert J., Ferguson, Kyle J., Webb, Gregory E., Feng, Yue-xing, Higgins, Pennilyn, Nguyen, Ai Duc, Zhao, Jian-xin, Joannes-Boyau, Renaud, Louys, Julien, 2017. Seasonal migration of marsupial megafauna in Pleistocene Sahul (AustraliaeNew Guinea). Proc. R. Soc. B. 284, 20170785.

Price, G.J., Louys, J., Cramb, J., Feng, Y.-x., Zhao, J.-x., Hocknull, S.A., Webb, G.E., Nguyen, A.D., Joannes-Boyau, R., 2015. Temporal overlap of humans and giant lizards (Varanidae; Squamata) in Pleistocene Australia. Quat. Sci. Rev. 125, 98-105.

Puaud, S., Nowak, M., Pont, S., Moncel, M.-H., 2015. Minéraux volcaniques et alpins à l'abri du Maras (Ardèche, France) : témoins de vents catabatiques dans la vallée du Rhône au Pléistocène supérieur. Comptes Rendus Palevol 14, 331-341.

Quiles, A., Valladas, H., Bocherens, H., Delqué-Količ, E., Kaltnecker, E., van der Plicht, J., Delannoy, J.-J., Feruglio, V., Fritz, C., Monney, J., Philippe, M., Tosello, G., Clottes, J., Geneste, J.-M., 2016. A high-precision chronological model for the decorated Upper Paleolithic cave of Chauvet-Pont d'Arc, Ardèche, France. Proc. Natl. Acad. Sci. Unit. States Am. 113, 4670-4675.

Quiles, A., Valladas, H., Geneste, J.M., Clottes, J., Baffier, D., Berthier, B., Brock, F., Bronk Ramsey, C., Delqué-Koliˇc, E., Dumoulin, J.P., Hajdas, I., Hippe, K., Hodgins, G.W.L., Hogg, A., Jull, A.J.T., Kaltnecker, E., de Martino, M., Oberlin, C., Petchey, F., Steier, P., Synal, H.A., van der Plicht, J., Wild, E.M., Zazzo, A., 2013. Second radiocarbon intercomparison program for the chauvet-pont d'Arc cave, Ardèche, France. Radiocarbon 56, 883-850.

Rae, A.M., Ivanovich, M., 1986. Successful application of uranium series dating of fossil bone. Appl. Geochem. 1, 419-426.

Raynal, J.-P., Moncel, M.-H., Fernandes, P., Bindon, P., Daujeard, C., Fiore, I., Santagata, C., Lecorre-Le Beux,

M., Guadelli, J.-L., Lepape, J.M., Liabeuf, R., Servant, L., Aulanier, M., Seret, H., 2013a. From Lower to Middle Palaeolithic in the South-East portion of the French Massif Central : land-cognition and use, related tool-kits and archaeo-ethnographical perspectives. Quartar 60, 29-59.

Raynal, J., Moncel, M., Fernandes, P., Bindon, P., Daujeard, C., Fiore, I., Santagata, C., Lecorre-Le Beux, M., Guadelli, J., Lepape, J., 2013b. From Lower to Middle Palaeolithic in the South-East portion of the French Massif Central: land-cognition and use, related tool-kits and archaeo-ethnographical perspectives. Quartar 60, 29-59.

Richard, M., Falguères, C., Pons-Branchu, E., Bahain, J.J., Voinchet, P., Lebon, M., Valladas, H., Dolo, J.M., Puaud, S., Rué, M., Daujeard, C., Moncel, M.H., Raynal, J.P., 2015. Contribution of ESR/U-series dating to the chronology of late Middle Palaeolithic sites in the middle Rhône valley, southeastern France. Quat. Geochronol. 30, 529-534.

Rivals, F., Moncel, M.-H., Patou-Mathis, M., 2009. Seasonality and intra-site variation of Neanderthal occupations in the Middle Palaeolithic locality of Payre (Ardèche, France) using dental wear analyses. J. Archaeol. Sci. 36, 1070-1078.

Rufà, A., Blasco, R., Roger, T., Moncel, M.-H., 2016. What is the taphonomic agent responsible for the avian accumulation? An approach from the Middle and early Late Pleistocene assemblages from Payre and Abri des Pêcheurs (Ardèche, France). Quat. Int. 421, 46-61.

Sadier, B., 2013. In: 3D et géomorphologie karstique : La grotte Chauvet et les cavités des Gorges de l'Ardèche. PhD thesis. Université de Grenoble, p. 478.

Sambridge, M., Grün, R., Eggins, S., 2012. U-series dating of bone in an open system: the diffusion-adsorption-decay model. Quat. Geochronol. 9, 42-53.

Sartégou, A., Bourlès, D.L., Blard, P.-H., Braucher, R., Tibari, B., Zimmermann, L., Leanni, L., Aumaître, G., Keddadouche, K., 2018. Deciphering landscape evolution with karstic networks: a Pyrenean case study. Quat. Geochronol. 43, 12-29.

Smith, T.M., Austin, C., Green, D.R., Joannes-Boyau, R., Bailey, S., Dumitriu, D., Fallon, S., Grün, R., James, H.F., Moncel, M.-H., Williams, I.S., Wood, R., Arora, M., 2018. Wintertime stress, nursing, and lead exposure in Neanderthal children. Science Advances 4, eaau9483.

St Pierre, E.J., Zhao, J.-x., Feng, Y.-x., Reed, E., 2012. U-series dating of soda straw stalactites from excavated deposits: method development and application to Blanche Cave, Naracoorte, South Australia. J. Archaeol. Sci. 39, 922-930.

St Pierre, E., Zhao, J.-x., Reed, E., 2009. Expanding the utility of Uranium-series dating of speleothems for archaeological and palaeontological applications. J. Archaeol. Sci. 36, 1416-1423.

Szmidt, C.C., Moncel, M.-H., Daujeard, C., 2010. New data on the late mousterian in mediterranean France:

first radiocarbon (AMS) dates at Saint-Marcel cave (Ardèche). Comptes Rendus Palevol 9, 185-199.

Tassy, A., Mocochain, L., Bellier, O., Braucher, R., 2013. Coupling cosmogenic dating and magnetostratigraphy to constrain the chronological evolution of peri-Mediterranean karsts during the Messinian and the Pliocene: example of Ardèche valley, Southern France. Geomorphology 81-92.

Tissoux, H., Falguères, C., Voinchet, P., Toyoda, S., Bahain, J.J., Despriée, J., 2007. Potential use of Ti-center in ESR dating of fluvial sediment. Quat. Geochronol. 2, 367-372.

Toffolo, M.B., 2021. The significance of aragonite in the interpretation of the microscopic archaeological record. Geoarchaeology 36, 149-169.

Toyoda, S., Voinchet, P., Falguères, C., Dolo, J.M., Laurent, M., 2000. Bleaching of ESR signals by the sunlight: a laboratory experiment for establishing the ESR dating of sediments. Appl. Radiat. Isot. 52, 1357-1362.

Tuffreau, A., 1993. In: Riencourt-lès-Bapaume (Pas-de-Calais). Un Gisement Paléolithique Moyen, , Documents d'Archéologie françaisevol. 37. Maison des sciences de l'homme, Paris, p. 126.

Valladas, H., Clottes, J., Geneste, J.M., Garcia, M.A., Arnold, M., Cachier, H., Tisnerat- Laborde, N., 2001. Palaeolithic paintings: evolution of prehistoric cave art. Nature 413, 479.

Valladas, H., Mercier, N., Ayliffe, L.K., Falguères, C., Bahain, J.J., Dolo, J.M., Froget, L., Joron, J.L., Masaoudi, H., Reyss, J.L., Moncel, M.H., 2008. Radiometric dates for the middle palaeolithic sequence of Payre (ardèche, France). Quat. Geochronol. 3, 377-389.

Vandenberghe, D., De Corte, F., Buylaert, J.P., Kuˇcera, J., Van den haute, P., 2008. On the internal radioactivity in quartz. Radiat. Meas. 43, 771-775.

Verna, C., Détroit, F., Kupczik, K., Arnaud, J., Balzeau, A., Grimaud-Hervé, D., Bertrand, S., Riou, B., Moncel, M.-H., 2020. The middle Pleistocene hominin mandible from Payre (ardèche, France). J. Hum. Evol. 144, 102775.

Vettese, D., Daujeard, C., Blasco, R., Borel, A., Caceres, I., Moncel, M.H., 2017. Neandertal long bone breakage process: standardized or random patterns? The example of Abri du Maras (Southeastern France, MIS 3). J. Archaeol. Sci.: Report 13, 151-163.

Voinchet, P., Bahain, J.-J., Falguères, C., Laurent, M., Dolo, J., Despriée, J., Gageonnet, R., Chaussé, C., 2004. ESR dating of quartz extracted from Quaternary sediments application to fluvial terraces system of northern France. Quaternaire 15, 135-141.

Yokoyama, Y., Falguères, C., Quaegebeur, J.P., 1985. ESR dating of quartz from quaternary sediments: first attempt. Nucl. Tracks Radiat. Meas. 10 (1982), 921-928.